Received: 4 January 2024 | Revised: 4 May 2024 | Accepted: 18 June 2024

DOI: 10.1002/joc.8551

RESEARCH ARTICLE

International Journal of Climatology RMetS

Recent and near-term future changes in impacts-relevant seasonal hydroclimate in the world's Mediterranean climate regions

Richard Seager[1] | **Yutian Wu**[1] | **Annalisa Cherchi**[2] | **Isla R. Simpson**[3] | **Timothy J. Osborn**[4] | **Yochanan Kushnir**[1] | **Jelena Lukovic**[5] | **Haibo Liu**[1] | **Jennifer Nakamura**[1]

[1]Lamont Doherty Earth Observatory of Columbia University, Palisades, New York, USA

[2]Istituto di Scienze dell'Atmosfera e del Clima, Bologna, Italy

[3]NSF National Center for Atmospheric Research, Boulder, Colorado, USA

[4]Climatic Research Unit, University of East Anglia, Norwich, UK

[5]University of Belgrade, Belgrade, Serbia

Correspondence
Richard Seager, Lamont Doherty Earth Observatory of Columbia University, Palisades, NY 10964, USA.
Email: seager@ldeo.columbia.edu

Funding information
NSF, Grant/Award Numbers: AGS-2127684, 1852977; European Union's Horizon Europe research and innovation programme under OptimESM, Grant/Award Number: 101081193

Abstract

Change over recent decades in the world's five Mediterranean Climate Regions (MCRs) of quantities of relevance to water resources, ecosystems and fire are examined for all seasons and placed in the context of changes in large-scale circulation. Near-term future projections are also presented. It is concluded that, based upon agreement between observational data sets and modelling frameworks, there is strong evidence of radiatively-driven drying of the Chilean MCR in all seasons and southwest Australia in winter. Observed drying trends in California in fall, southwest southern Africa in fall, the Pacific Northwest in summer and the Mediterranean in summer agree with radiatively-forced models but are not reproduced in a model that also includes historical sea surface temperature (SST) forcing, raising doubt about the human-origin of these trends. Observed drying in the Mediterranean in winter is stronger than can be accounted for by radiative forcing alone and is also outside the range of the SST-forced ensemble. It is shown that near surface vapour pressure deficit (VPD) is increasing almost everywhere but that, surprisingly, this is contributed to in the Southern Hemisphere subtropics to mid-latitudes by a decline in low-level specific humidity. The Southern Hemisphere drying, in terms of precipitation and specific humidity, is related to a poleward shift and strengthening of the westerlies with eddy-driven subsidence on the equatorward side. Model projections indicate continued drying of Southern Hemisphere MCRs in winter and spring, despite ozone recovery and year-round drying in the

Mediterranean. Projections for the North American MCR are uncertain, with a large contribution from internal variability, with the exception of drying in the Pacific Northwest in summer. Overall the results indicate continued aridification of MCRs other than in North America with important implications for water resources, agriculture and ecosystems.

KEYWORDS

atmospheric circulation, climate change, hydroclimate, Mediterranean-type climates

1 | INTRODUCTION

The world's Mediterranean climate regions (MCRs) occupy transitional zones between the subtropics and mid-latitudes on the western edges of continents. The Mediterranean climate type is characterized by temperate, wet winters and hot or warm dry summers. The wet winters arise from MCRs being on the equatorward flank of the mid-latitude storm tracks and just poleward of the descending branch of the Hadley Cell. In summer the storm tracks retreat poleward, monsoons develop over land and subtropical highs expand poleward and intensify over the oceans, while the Hadley Cell straddles the Equator with descent in the winter hemisphere (Chen et al., 2001; Rodwell & Hoskins, 2001; Seager et al., 2003). The dry summers arise from the MCRs being on the eastern flanks of the subtropical highs with equatorward, subsiding flow that suppresses precipitation. Spring and fall are transitional seasons between these winter and summer states. This faithfully describes the mean climates of the west coast of the United States and Baja, Mexico, Chile, Portugal and Morocco, southwest South Africa and southwest Australia (Alessandri et al., 2014; Deitch et al., 2017). The lands along the northern and southern shores of the Mediterranean Sea and the Middle East also have a Mediterranean-type climate but this is unique amongst the MCRs. In this case, it is the winter Mediterranean Sea storm track, rather than the North Atlantic storm track, that provides winter precipitation (Lionello et al., 2006; Seager et al., 2014; Zappa et al., 2015a) while summer high pressure extends well east of the North Atlantic subtropical high in part related to descent induced by the Asian monsoon and interactions with orography (Rodwell & Hoskins, 2001; Simpson et al., 2015). Southcentral to southeastern Australia also has a somewhat unique Mediterranean zonally-extended climate that has been less well studied but can possibly be explained in terms of the zonal orientation of the coast and the equatorward movement in winter, and poleward movement in summer, of the zonally-oriented Southern Hemisphere storm track as shown in Seager et al. (2019b, hereafter S19).

The stark seasonality and the hot summers create a climate that borders on semi-arid and one in which there are frequent hydrological disruptions in terms of heavy precipitation and drought. California is a good example which in this century has already experienced one of the worst extended droughts on record (Seager et al., 2015; Swain et al., 2014) and a very wet winter in 2022/23. Chile has been been enduring a recent multiyear drought. Precipitation in both California and Chile is influenced by the El Niño–Southern Oscillation and its decadal companion, the Pacific Decadal Oscillation, via Rossby wave teleconnections and shifts in the jet streams and storm tracks (Maher et al., 2022; Seager et al., 2005). The recent Chilean extended drought has however been connected to subtropical South Pacific Ocean variability (Garreaud et al., 2018). Cape Town has also recently endured its record-breaking "Day Zero" drought (Burls et al., 2019; Pascale et al., 2020; Sousa et al., 2018).

Drought and water availability are always concerns across all the MCRs and have serious social impacts since all of the MCRs are home to large cities and locally and globally important agricultural production (olives, citrus, grapes, grains, nuts, etc.). In addition, the MCRs face considerable fire hazard and ecological changes that are influenced by climate change (Jones et al., 2022). Water resources rely heavily on cool season precipitation but fire and ecosystem impacts depend on both cool season precipitation and vapour pressure deficit (VPD—the difference between saturation and actual vapour pressure and a measure of atmospheric aridity), and, hence, air temperature and humidity, from spring into summer (Goss et al., 2020; Jacobson et al., 2022; Williams et al., 2015, 2019).

From the climate dynamics point of view, an-all MCRs perspective is useful (Alessandri et al., 2014; Polade et al., 2017, S19). The location of the MCRs suggests that climate variability and change might be influenced, in winter, by changes in the extratropical storm tracks and Hadley Cell extent and intensity (Grise et al., 2019) and, in summer, by changes in subtropical highs (Cherchi et al., 2018; He et al., 2017) and monsoons. The spring and fall seasons could be influenced by

changes in the seasonal cycle of these different circulation regimes. However, the Northern Hemisphere has strong winter stationary waves which might introduce zonal (Simpson et al., 2016) and inter-hemispheric asymmetries that complicate this picture. Further, in terms of anthropogenic forcing, the Southern Hemisphere has been more strongly influenced by stratospheric ozone depletion and the beginning of recovery than has the Northern Hemisphere (Polvani et al., 2011) and this should create inter-hemisphere asymmetry in the amplitude and seasonal cycle of forced responses. Further, the North American and Chile MCRs are influenced by tropical Pacific SST variations but the other MCRs are less obviously influenced by SSTs anywhere (S19). Consequently, a comparative study of the MCRs draws attention to the physical mechanisms of variability and change that drive similarities and differences between hemispheres and longitudes.

Here we will focus on observed hydroclimate change in the five MCRs over past decades and model-projected change over coming decades, all with reference to the large-scale circulation changes involved. The paper is conceived as partly a review and hence structured somewhat unusually. Unlike a review, we will first conduct new analysis of past and model-projected trends. Since considerable work has been done on winter and summer change (for some recent work, see, e.g., S19; Tuel et al., 2021; Zappa et al., 2015b), but spring and fall can be important in terms of ecology and length and severity of wildfires, we will focus more on change during these transition seasons. We will also examine changes in precipitation but, motivated by the importance of fire, we will examine trends over past decades in low-level and surface specific humidity and VPD in the spring. This will reveal a surprising and widespread atmospheric drying in many subtropical to mid-latitude regions capable of influencing the MCRs, as has also been noted recently by Simpson et al. (2023) and Jacobson et al. (2023), with implications for enhancement of fire hazard. Precipitation and humidity trends will be related to changes in large-scale circulation. The analysis will include observations, reanalyses, SST-forced atmosphere models and radiatively-forced coupled climate models. After this, we will critically discuss at length the research to date on past and future hydroclimate trends in MCRs and the mechanisms for these that have been invoked. We aim to provide an up-to-date account of ongoing change in impacts-relevant aspects of the hydroclimate of MCRs, place this in a large-scale dynamical context and then consider what we can say about near-term future change and critically discuss the mechanisms proposed to explain these past and future changes. Although we do not quantify it here, the changes we identify will be useful for considering how MCRs shift poleward over the coming decades (Alessandri et al., 2014).

2 | OBSERVATIONAL DATA, REANALYSES, MODELS AND METHODS

2.1 | Observations-based datasets

For observational, station-based, precipitation we use the Climatic Research Unit (CRU) TS4.06 data (Harris et al., 2020) and available at https://crudata.uea.ac.uk/cru/data/hrg/ and the Global Precipitation Climatology Center (GPCC) data (Schneider et al., 2014) available at https://www.ncei.noaa.gov/products/land-based-station/global-historical-climatology-network-daily. Over North America we additionally make use of the PRISM data (Daly et al., 2008) available at https://prism.oregonstate.edu. For estimates of the vapour pressure and historical circulation trends we use the European Centre for Medium Range Weather Forecasts Reanalysis 5 (ERA5; Hersbach et al., 2020) available at https://www.ecmwf.int/en/forecasts/dataset/ecmwf-reanalysis-v5. Both Jacobson et al. (2023) and Simpson et al. (2023) have validated the ERA5 lower atmosphere humidity trends against in situ data and shown it to be qualitatively and quantitatively reliable. The period of analysis was from 1959 to 2021. While ERA5 begins earlier we had some concerns about data reliability in the 1950s. The chosen period is 62 years which is long enough for most forced trends to emerge from the "noise" of interannual to decadal variability.

2.2 | Coupled model simulations

We also examine the coupled model simulations from Coupled Model Intercomparison Project 6 (CMIP6; Eyring et al., 2016) using the "historical" simulations with estimated changes in radiative forcing and land use cover and change to 2014 and the projections with the SSP370 scenario from 2015 to 2050 and obtained from https://esgf-node.llnl.gov/projects/cmip6/. This scenario has greenhouse gas emissions that are less than the highest scenario but still represents radiative forcing increasing to 7 $W \cdot m^{-2}$ by 2100. In the near-term of committed warming that we focus on, climate change is not strongly dependent on the choice of emissions scenario since these diverge more importantly later in the century. In the presence of significant adoption of renewable fuels in many countries, but lack of any internationally enforceable agreements to reduce GHG emissions, we

consider it a realistic projection for the next few decades. However, it should be noted this is also a high aerosols emissions scenario (Shiogama et al., 2023). We used all runs of all models with the data needed available. The radiatively-forced response was computed as the mean of the ensemble means for each model, thus providing each model equal weight. In addition, for uncertainty analysis, we make use of 10 large model ensembles with CMIP5 (RCP8.5 forcing scenario) and 6 (SSP585 forcing scenario) generation models: CanESM2, CSIRO-Mk3-6-0, GFDL-CM3, MPI-ESM, CESM1-CAM5, ACCESS-ESM1-5, CanESM5, EC-Earth3, MIROC6 and MPI-ESM1-2-LR (data available at the multimodel large ensemble repository https://www.cesm.ucar.edu/community-projects/mmlea). The first 20 members from each large ensemble were used, which is large enough for the ensemble mean to isolate that model's radiatively-forced change.

2.3 | Atmosphere model forced by observed SSTs

In addition, we use a 10-member ensemble of Community Atmosphere Model 6 (CAM6) forced by observed SST and SSP370 radiative forcing and land cover change covering the 1959–2021 period. The model was run by the National Center for Atmospheric Research (NCAR) who make the data available at https://www.cesm.ucar.edu/working-groups/climate/simulations/cam6-prescribed-sst where more details are provided about the model simulations. The ensemble mean of this model identifies the response to the imposed SST plus radiative forcing and land use change.

2.4 | Methods

Trends are computed by linear least squares regression and statistical significance is assigned according to the 95% confidence level using a two-sided *t* test. For models we assess agreement as 75% of model ensemble means agreeing on the sign of trend or change and agreeing with the multimodel ensemble mean sign of trend or change. Trends are plotted in units of the variable (e.g., mm·month^{-1} for precipitation) change over the 1959–2021 period. Qualitatively very similar results were obtained using Sen's slope estimator and a Mann–Kendal test with a 0.1 tolerance for probability of rejecting the null hypothesis of no monotonic-trend.

We examine the uncertainties in precipitation projections and the relative importance of internal variability and model response uncertainty by considering the 10 large ensembles. To investigate the role of internal variability and model response uncertainty in contributing to uncertainty in future projections we follow the methods of Hawkins and Sutton (2009, 2011) and Lehner et al. (2020) to partition the 90% confidence interval (following from what is used in Hawkins & Sutton, 2009) into these two components, neglecting the small scenario differences between the RCP8.5 and SSP5-8.5 scenarios. The 90% uncertainty ranges are computed additively and symmetrically around the multi-model ensemble mean. The ensemble mean for each model averages across the uncorrelated internal variability in each member and isolates the forced response common to each ensemble member. By the same reasoning, the departure of each ensemble member for a model from the ensemble mean for that model isolates the internal variability. The overall 90% confidence interval on the large ensembles is computed as $1.654^{*}\left(\sqrt{(M)}+\sqrt{(I)}\right)/F$, where $F=\left(\sqrt{(M)}+\sqrt{(I)}\right)/\sqrt{(M+I)}$, the model response component is computed as $\pm 1.654^{*}\sqrt{(M)/F}$ and the internal variability component is the remainder. Here, M refers to the variance across the 10 model ensemble means (which represents the model response component) and I is the average, across models, of the variance across ensemble members for a given model (which represents the internal variability component). An assumption is made here that the uncertainties due to model response differences and internal variability are distributed normally and symmetrically around the ensemble mean, which is an approximation. To provide an assessment of the extent to which this approximation is valid, we also directly compute the 90% confidence interval across the large ensemble members as the 5th to 95th percentile range across all members from all models. In most regions, except for South Africa where there is an outlying model, this 90% confidence interval agrees well with that computed using the above decomposition.

2.5 | Definition of MCRs and regional averages

To identify MCRs we used the Köppen climate classifications *Csa* and *Csb* which are the hot and warm summer Mediterranean climate types, respectively. The categorization is that of Leemans and Cramer (1991) and is provided with details at http://iridl.ldeo.columbia.edu/SOURCES/.UN/.FAO/.NRMED/.SD/.Climate/.dataset_documentation.html#anchor2. Area averages are over these climate classifications. The red boxes shown in Figures 1 and 2 are merely to draw attention to the MCRs within them. The MCR regions remain fixed over historical and future time. The fact that MCRs in reality will be

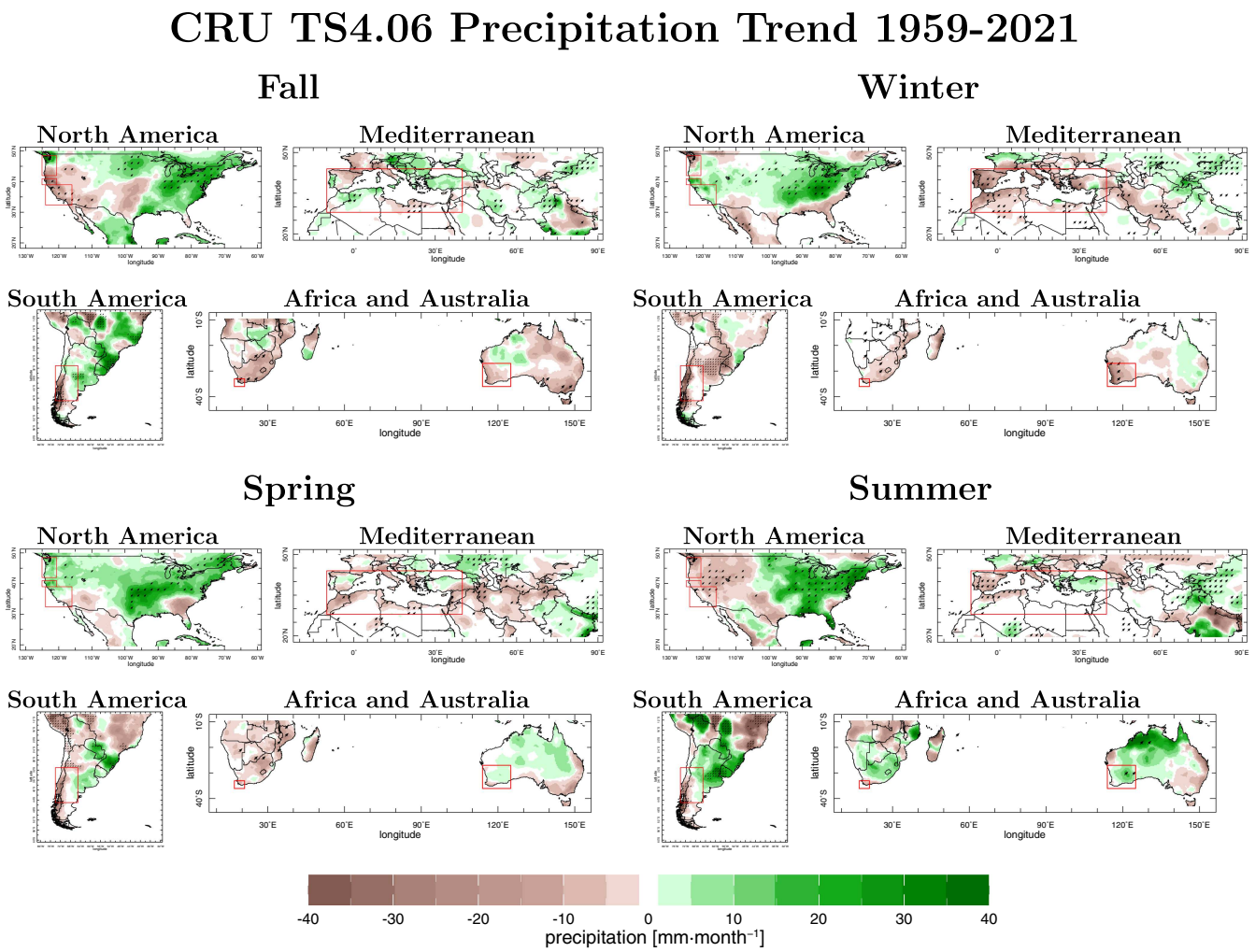

FIGURE 1 Observed trends in precipitation for fall, winter, spring and summer, as labelled, and for all MCRs. Stippling indicates significance at the 5% level. Units are mm·month^{-1} change over the 1959–2021 period.

expected to move over the coming decades, with parts of the current MCRs transitioning into different climate types, will be briefly discussed in section 6.

3 | OBSERVED AND RADIATIVELY-FORCED MODELLED TRENDS OVER THE PAST SIX DECADES

3.1 | Observed and radiatively-forced modelled precipitation trends across seasons in the world's MCRs

In Figure 1 we show observed trends in CRU precipitation over 1959 to 2021 for fall, winter, spring and summer seasons, focusing on the MCRs and their surrounding regions. Winter trends have already been examined by S19 and the addition of three more years here does not change the story: the west coast of North America is unique in having a winter wetting trend while the other four MCRs have experienced winter drying and, of these, the drying in much of the Mediterranean, Chile and southwest Australia is statistically significant. Looking at the other seasons, Chile stands out for having a statistically significant drying in all seasons. This also occurs in southwest Africa though not all at this level of significance. The Mediterranean region also has experienced statistically significant drying in parts of coastal North Africa and the Middle East in spring, in its western parts in Africa and Iberia in summer and in eastern Libya in fall. California has had a drying trend in the fall and all of the west coast of North America has in summer with much of these statistically significant. Statistically significant wetting trends in MCRs are limited to northwest Algeria in fall, northern Turkey in summer, and, in the

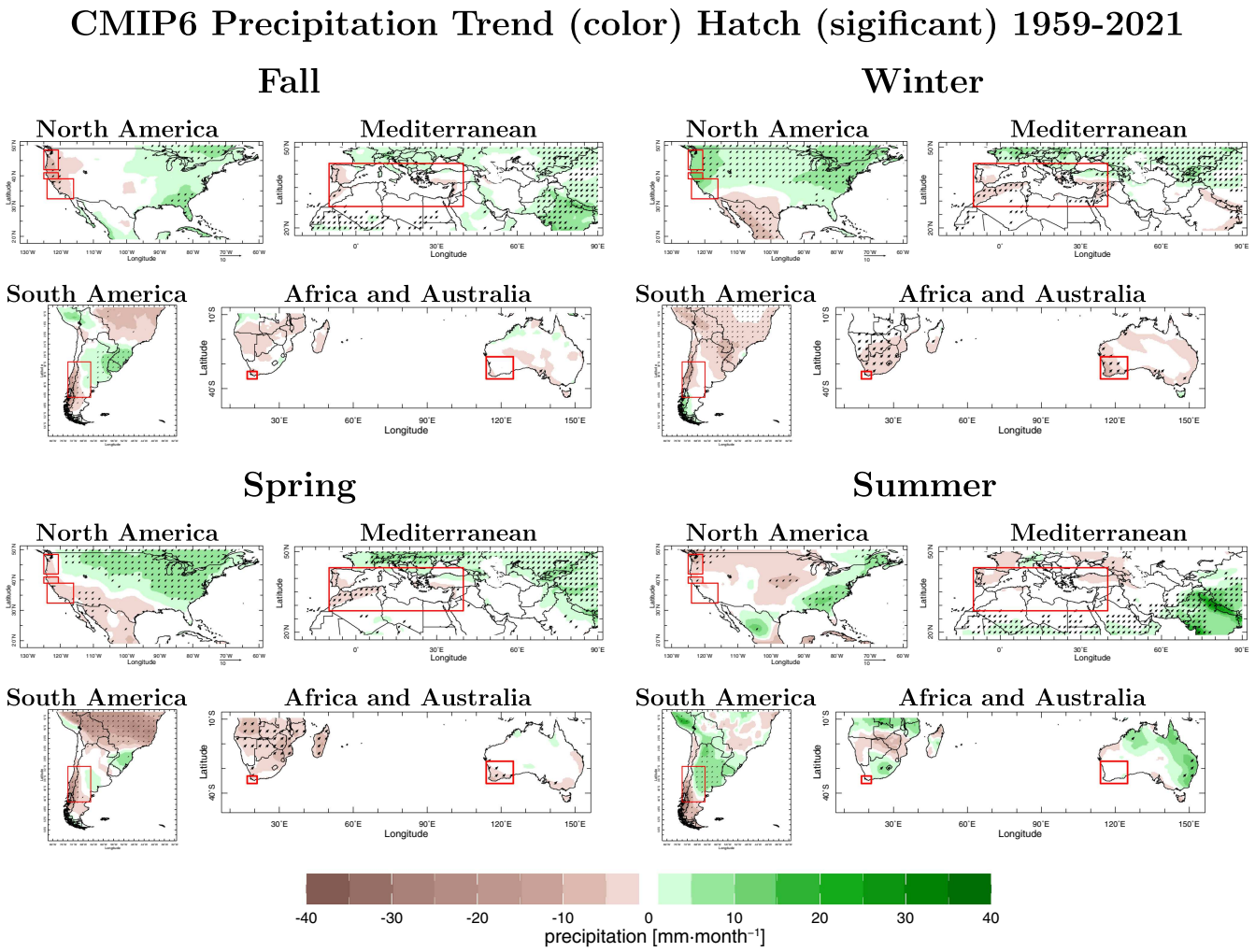

FIGURE 2 As in Figure 1 but for the ensemble mean of the CMIP6 historical and SSP370 simulations. Here stippling indicates 75% of models agree on sign of change and agree with the sign of the ensemble mean change.

Southern Hemisphere, just parts of southwest Australia in summer. Clearly, drying trends are much more common across MCRs in space and seasons than wetting trends but are not entirely ubiquitous. The Mediterranean region itself is large and could contain quite different trends across its area. However, more than 85% and 70% of grid points in the *Csa* and *Csb* areas have drying trends in winter and spring, respectively, considering CRU and GPCC data.

Figure 2 shows the CMIP6 multimodel mean radiatively-forced trends of precipitation over 1959–2021. Overall the model trends are weaker than observed. Looking at winter first and as discussed by S19, the models suggest that much of the Mediterranean and all the Southern Hemisphere MCRs should have dried over the past decades due to changes in radiative forcing while the west coast of North America should have got wetter. This agrees with the observed trends other than for the Pacific Northwest. The models also suggest all the Southern Hemisphere MCRs should have dried in all seasons other than southwest Australia in summer for which they show no trend. This is a remarkable agreement with the observed Southern Hemisphere MCR drying trends. For the Mediterranean, the models also indicate a spring and fall drying in parts of northwest Africa and Iberia and across the region in summer, although only some subregions reach significance. All of these modelled trends have occurred in observations with at least partial agreement in location. In the North American MCR the situation is curious: the models predict radiatively-driven drying in spring and summer and fall, which together with the increase in winter, translates into a shorter and sharper wet season. This model hindcast agrees with the observations in summer and in California in fall but disagrees in spring and in the Pacific Northwest in fall which have got wetter. For the large

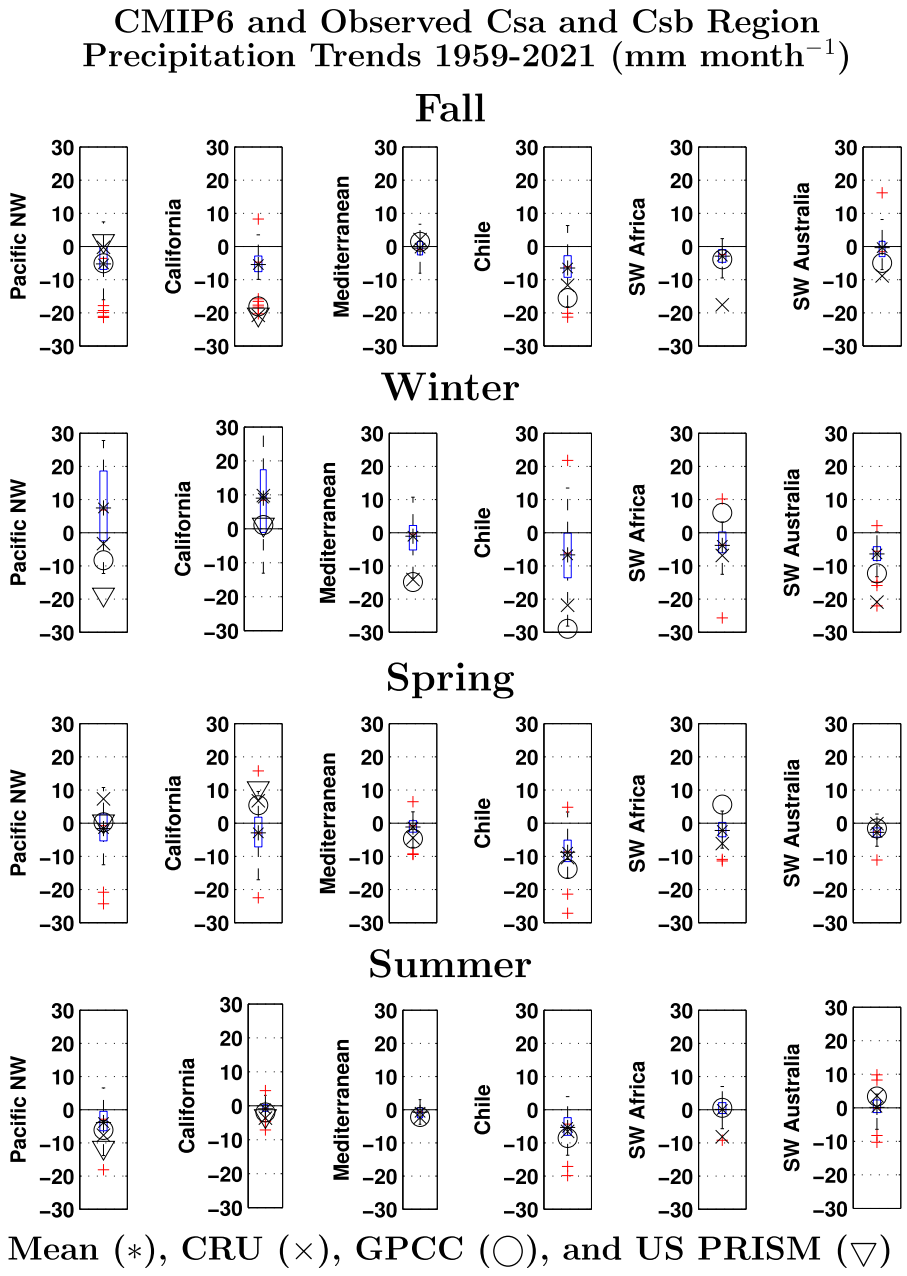

FIGURE 3 The observed and CMIP6 historical and SSP370 simulated trends in seasonal precipitation for 1959–2021 for each of the MCRs. The multimodel ensemble mean is marked by an asterisk. The edges of the box mark the 25th and 75th percentile of the ensemble spread across model ensemble means, the horizontal line is the median, the whiskers mark the range and outliers (beyond one and a half times the inter-quartile range from the 25th or 75th percentiles) are red crosses.

Mediterranean MCR, 60% in fall, 75% in winter, 78% in spring and 86% in summer of grid points have model-simulated drying.

Figure 3 shows these results in summary form for areal averages and adding in the GPCC observations and, for North America, the PRISM observations too. The model results are shown as box and whisker plots that represent the across-model ensemble means distributions with outliers marked. We will discuss the results by region reading from left to right across the columns in Figure 3. For the Pacific Northwest, the main source of agreement between models and observations (three data sets) is drying in the summer, while there is a disagreement between model-predicted wetting in winter and observed drying. For California, models and observations agree on drying in the fall, the wetting in winter in CRU agrees with model simulations but is not supported by the other two observational precipitation data sets (GPCC and PRISM) and model-simulated drying in spring disagrees with observed wetting. CRU and GPCC observational data sets agree on winter and spring drying in the Mediterranean region but, although the CMIP6 multimodel mean and median have a weaker drying in these seasons, many model runs also have wetting. Given the likelihood of internal variability contributing to the model spread, this suggests that the observed drying might have been contributed to by natural variability as well (see Kelley et al., 2011; Trigo et al., 2004; Xoplaki

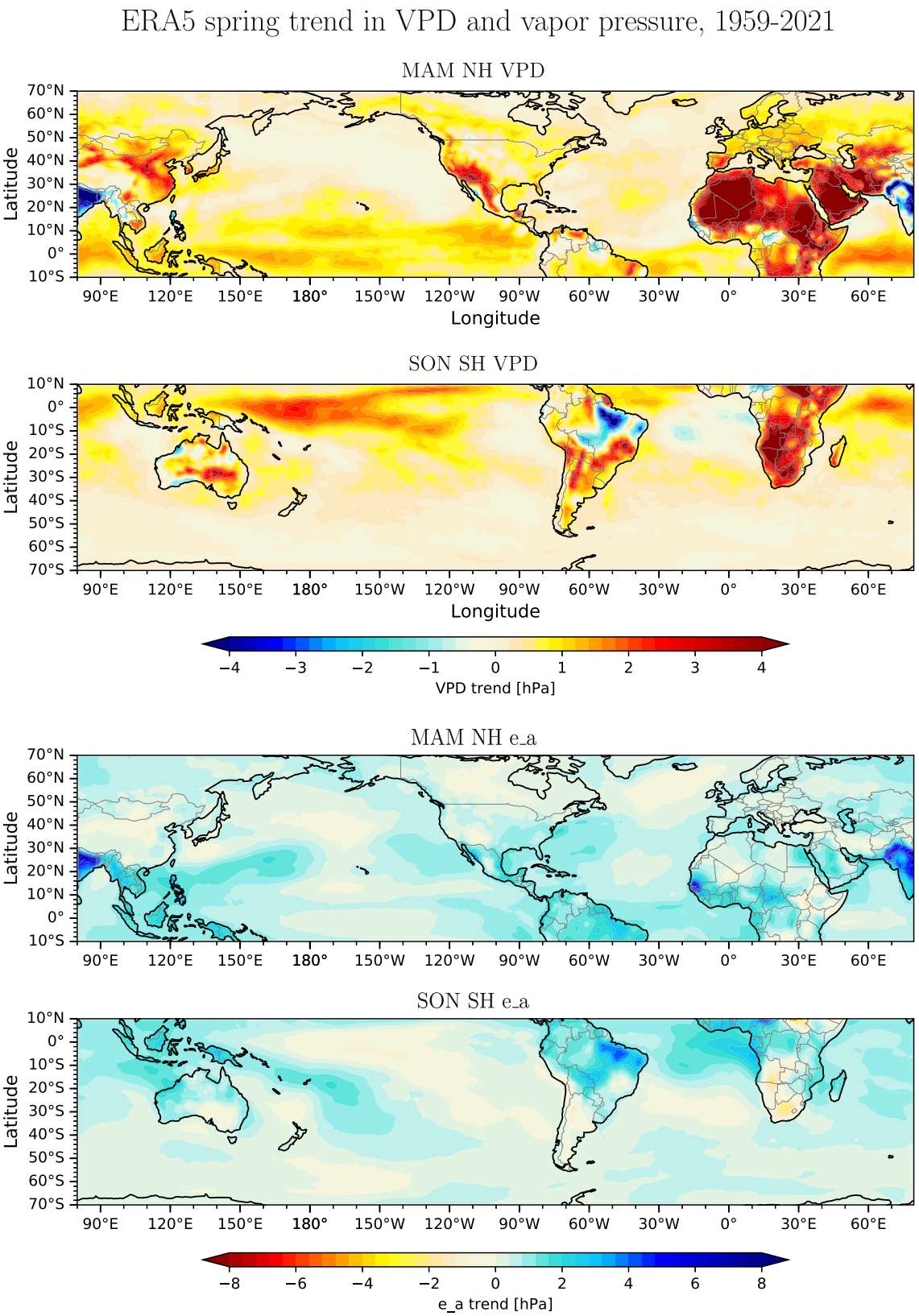

FIGURE 4 Trends in spring VPD (top two panels) and surface air humidity (bottom two panels), both in hPa, for the Northern Hemisphere and Southern Hemisphere. Note the wider colour scale for VPD than for air humidity.

et al., 2004) although it is also possible that models underestimate the precipitation response in the Mediterranean to GHG-forced circulation change (Zappa et al., 2015a). Chile is a standout—all seasons, observations and models robustly show drying providing a strong indication that this is a dramatic human-driven aridification. There is a similar agreement on southwest Africa in the fall. However, the strong drying that CRU shows here in other seasons is not seen in the GPCC data though the CMIP6 models do indicate a weak human-driven drying in winter and spring. Models and CRU data agree on drying in southwest Africa in winter and spring but GPCC data indicates wetting. For southwest Australia, models and observations agree on drying in winter, the observed fall drying is not found in the CMIP6 models, there is a hint of agreement on spring drying and the observed summer wetting is not found in the radiatively-driven response of CMIP6 models.

3.2 | Observed trends in spring humidity and VPD in and west of the world's MCRs

It has been shown for the North American MCR that high VPD preceding the summer fire season is associated with higher burned forest area (Jacobson et al., 2022). In that interannually varying case, the high VPD is contributed to by a statistically significant higher saturation vapour pressure but also, at lesser levels of statistical significance, by lower specific humidity. While this relation between fire and atmospheric aridity has not been proven in other areas, it motivates the next analysis of trends in VPD and specific humidity across the MCRs and their nearby ocean areas in the spring season. To start, the trend in spring VPD is shown in Figure 4. VPD is generally expected to increase since, due to the exponential dependence of saturation humidity on temperature, even constant relative humidity will lead to increasing VPD. Consistently we see rising VPD everywhere except over parts of the Amazon and the Indian subcontinent. Focusing on the MCRs, the VPD increase appears strikingly large in North America, Iberia and southwest Africa (as part of a general large increase across southern Africa).

Most of the increase in VPD is driven by atmospheric warming and rising saturation humidity (not shown) but of more surprise is that there are regions where the actual specific humidity is either not increasing or even slightly decreasing in ERA5 (Figure 4). Focusing on the MCR regions, there is a small area of specific humidity decrease—or no increase—in California and the interior southwest of the United States and also in central Iberia and parts of Morocco (see also Simpson et al., 2023). But these are relatively limited areas of the Northern Hemisphere where, otherwise, specific humidity rises as expected given warming and Clausius–Clapeyron constraints. More impressive is the widespread areas of decreasing specific humidity in the Southern Hemisphere subtropics. These lie west of, but impinging on, the southern MCRs in Chile, southwest Africa and southeastern Australia while southwest Australia does not appear to be affected in this way. Clearly, the surface specific humidity trend over the ocean will be related to the trend in SST. In the Southern Hemisphere this shows more regions of cooling or muted warming than the Northern Hemisphere with cooling across the Southern Ocean, over the southeast to eastern equatorial Pacific and muted warming in the South Atlantic (e.g., Heede & Federov, 2023; Wills et al., 2022). However, this is only a consistent relation and the SST trends themselves could be driven by the atmospheric humidity trends: in the absence of any other changes, reduced surface air humidity will tend to increase latent heat flux and cool the SST until the air–sea humidity difference and latent heat flux restore equilibrium at a lower SST (Betts & Ridgway, 1989).

3.3 | Association of changes in hydroclimate of MCRs with large-scale circulation

To check the association between specific humidity declines that impact Southern Hemisphere MCRs and the atmosphere circulation, in Figure 5 we show trends in the zonal mean zonal wind and transient eddy momentum flux $\overline{u'v'}$. These plots are shown for both hemispheres for context and contrast but our focus will be on the Southern Hemisphere. What jumps out is the strengthening of the Southern Hemisphere jet in every season which also is associated with a poleward shift in summer and, to some extent, fall. This is likely a response of the jet to increasing CO_2 and reducing O_3. In the Northern Hemisphere, where CO_2 forcing dominates, jet strengthening is weaker and restricted to winter alone. The Southern Hemisphere jet strengthening is associated with enhanced poleward transient eddy momentum fluxes immediately equatorward of the strengthening. Figure 6 then shows that the eddy momentum flux anomalies are associated with vertical motion anomalies with a trend towards subsidence in the subtropical to mid-latitude bands. These relationships can be understood in terms of a transient eddy-driven mean meridional circulation. An approximate zonal mean, denoted by angle brackets, zonal momentum equation can be written as $\partial\langle\overline{u}\rangle/\partial t - f\langle\overline{v}\rangle = -\partial\langle\overline{u'v'}\rangle/\partial y$ and the continuity

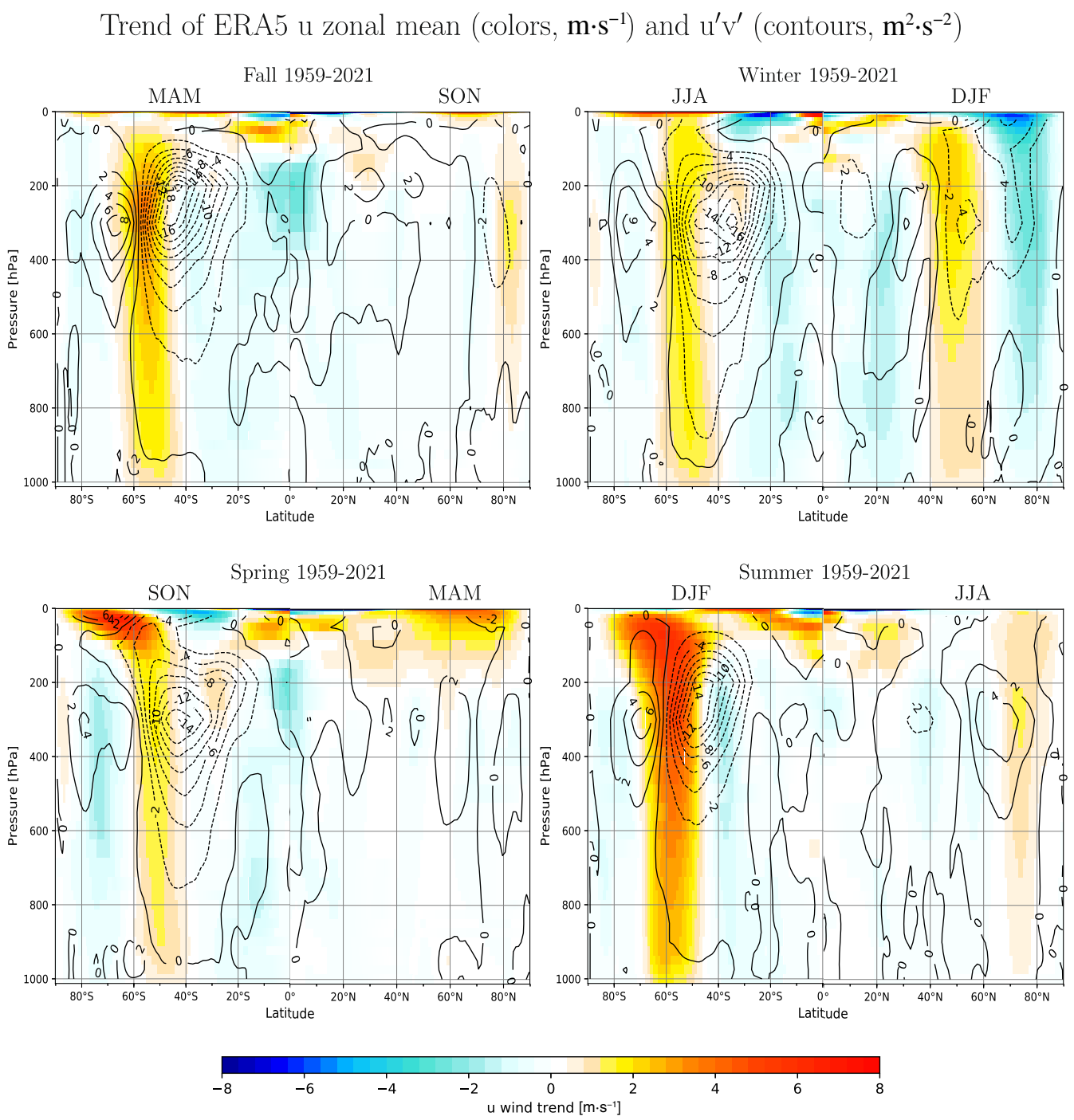

FIGURE 5 Trends in ERA5 zonal mean zonal wind (colours, $m \cdot s^{-1}$) and $\overline{u'v'}$ (contours, $m^2 \cdot s^{-2}$) for 1959–2021 for fall (top left), winter (top right), spring (bottom left) and summer (bottom right). Note that in each panel the appropriate season is shown for both hemispheres so fields shown are not continuous across the equator.

equation as $\partial\langle\overline{\omega}\rangle/\partial p = -\partial\langle\overline{v}\rangle/\partial y$. The trends towards enhanced poleward eddy momentum flux will tend to accelerate the jet on the poleward side and also induce an equatorward meridional flow. The meridional flow will drive subsidence on the equatorward flank of the enhanced eddy momentum flux. We propose that the eddy-induced subsidence causes the decline in specific humidity. Figure 7 supports this argument showing a general agreement in the Southern Hemisphere latitude-longitude domain between enhanced subsidence and drying of the lower troposphere in spring. Amidst general atmospheric wetting, there is a band of enhanced subsidence and lower troposphere drying centred around 30°C which is also

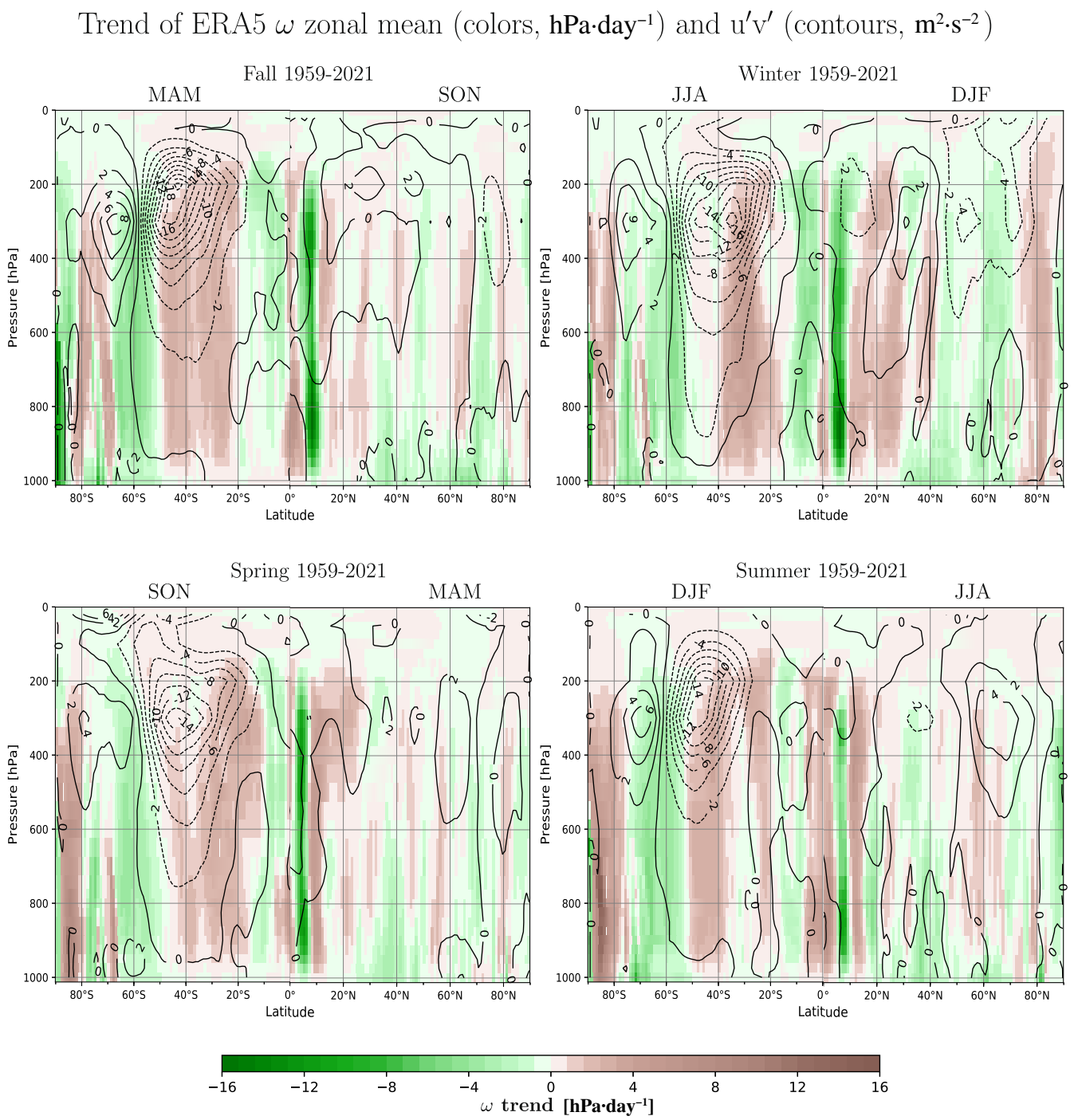

FIGURE 6 As in Figure 5 but for zonal mean vertical pressure velocity (colours, hPa·day^{-1}) and $\overline{u'v'}$ (contours, m^2·s^{-2}). Data plotted are for the same season (e.g., spring) in each hemisphere and hence are not continuous across the Equator.

enhanced immediately west of the South American and southwest African MCRs. (This causality is supported by a moisture budget decomposition as in S19 which is not shown here.) In the Northern Hemisphere there are similar features, notably in the subtropical Pacific, but these are not located to directly impact the MCRs.

3.4 | Observed, radiatively-forced and SST-forced trends in spring and fall

The observed trends in precipitation and circulation in spring and fall in the Northern Hemisphere and Southern Hemisphere could be driven by radiative forcing or arise from internal climate variability, including that in which

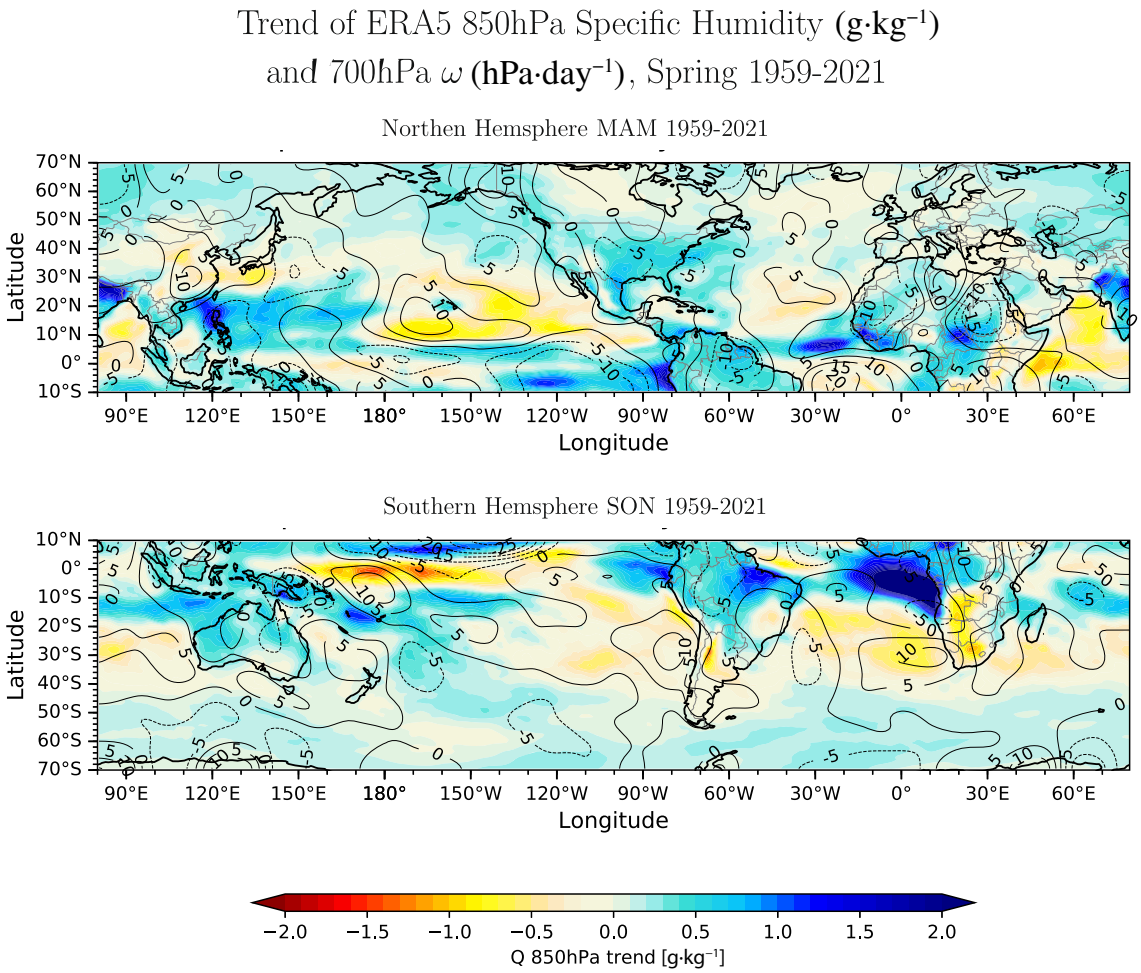

FIGURE 7 Trends over 1959–2021 in ERA5 850 hPa specific humidity (g·kg^{-1}, colour) and 700 hPa vertical pressure velocity (hPa·day^{-1}, contours) during spring (MAM for Northern Hemisphere and SON for Southern Hemisphere).

the atmosphere is driven by the ocean through SST trends. To look at this, Figures 8 and 9 show trends in SST, precipitation and 700 hPa heights in spring and fall as observed, in the ensemble mean of the SST-forced atmosphere model, and in the multimodel ensemble mean of the CMIP6 ensemble. In the Northern Hemisphere spring and fall it is difficult to attribute causality to the observed changes. In spring (Figure 8, left column) there has been a trend towards a deeper North Pacific low which is consistent with wetting on the west coast of North America north of California but the SST-forced model produces a trend towards higher pressure while CMIP6 has a considerably weaker increase in pressure centred over the western to central North Pacific. The coupled model that contains CAM6 is CESM2 and it also has a trend towards a North Pacific high though slightly to the west of its SST-forced counterpart (not shown). In northern spring the weak drying over the Mediterranean is associated with quite different circulation trends in observations and the SST-forced model (which is matched in CESM2) and there is almost no circulation trend in CMIP6.

In northern fall (Figure 9, left column) the agreement between observations and CMIP6 on drying of the North American MCR and a high over the North Pacific might encourage the interpretation that this is radiatively forced. However, the SST-forced model simulates a higher zonal wavenumber low–high–low pattern across the North Pacific and into North America which questions this. CESM2, however, simulates a trend towards a North Pacific high akin to CMIP6 (not shown). Consequently, the CAM6 high zonal wavenumber pattern is a response to the observed SST trend. In fall there is also little coherency between observed, SST-forced (or CESM) and CMIP6 circulation trends over the Mediterranean.

The situation is far less ambiguous in the Southern Hemisphere than in the Northern Hemisphere. In spring (Figure 8, right column) and fall (Figure 9, right column) the observed drying in the MCRs (although including just the far southwestern tip of Australia in spring) is

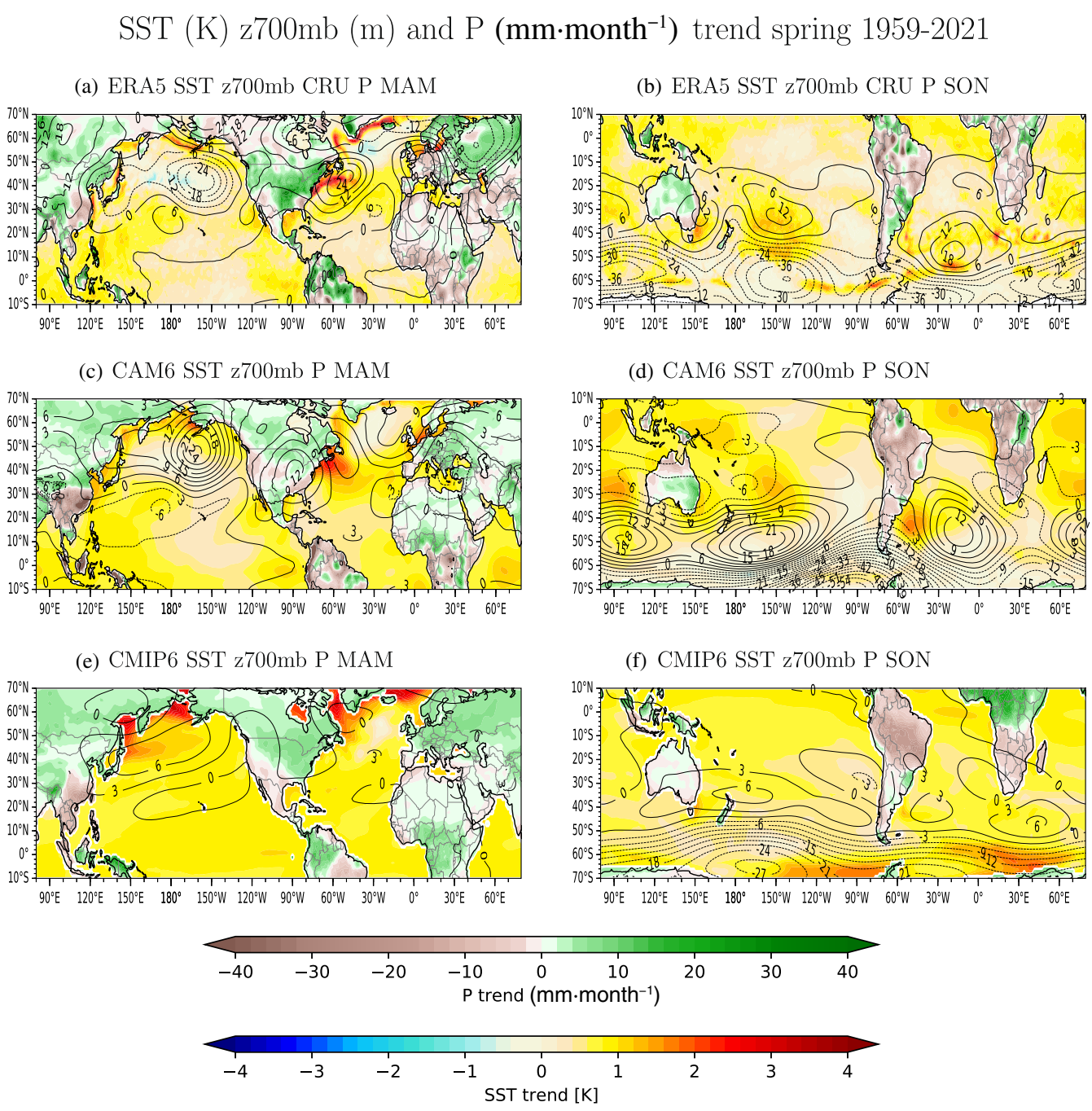

FIGURE 8 Trends over 1959–2021 in SST (colour, ocean), 700 hPa heights (contours) and precipitation (colours, land) for (top) ERA5 and CRU observations, (middle) the SST-forced CAM6 model and (bottom) the CMIP6 multimodel ensemble mean of coupled models for spring in the northern (left column) and southern (right column). For ERA5 and CAM6 the SST fields are observed estimates. Units are K for SST, m for heights and mm·month^{-1} for precipitation and represent that change over the trend period.

reproduced in both the SST-forced and CMIP6 models. This is associated with, allowing for disagreements on the details, trends towards increasing heights in the subtropics to mid-latitudes and lowering heights poleward. This trend is itself associated with the poleward shift of the westerlies and, according to the arguments above, subsidence and drying on the equatorward flank where the MCRs are. The SST trend includes that which is a response to radiative forcing but additionally includes any due to internal variability. The agreement across model experiments and across the Southern Hemisphere in spring and fall on circulation and MCR drying trends strongly indicates that human-induced radiative forcing of hydroclimate change has dominated the trends over the past half-century or so.

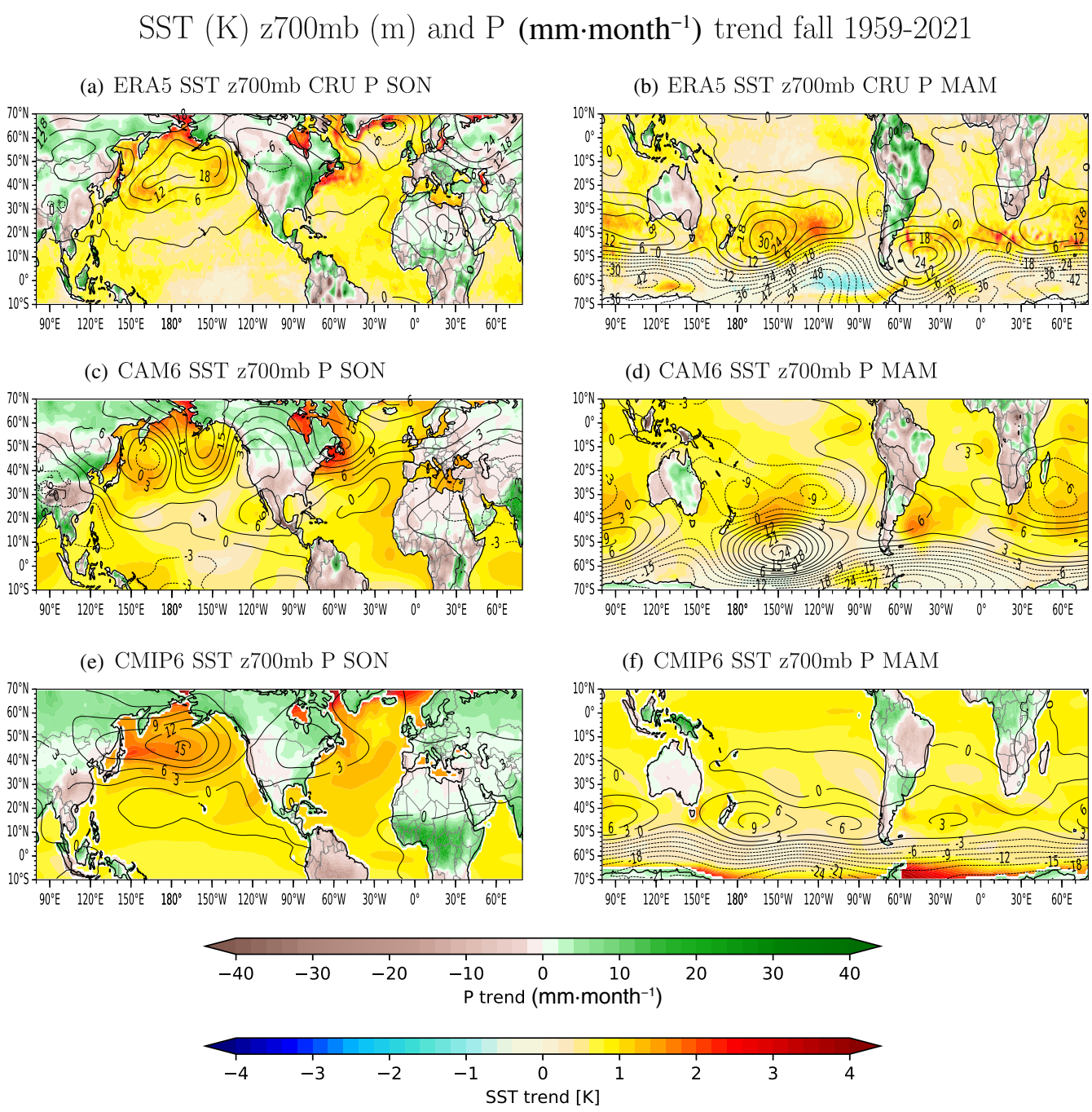

FIGURE 9 As in Figure 8 but for fall.

4 | MODEL-PROJECTED TRENDS OVER THE NEXT TWO DECADES IN SEASONAL PRECIPITATION IN THE WORLD'S MCRs

Given problems with CMIP6 models reproducing observed trends in surface and low-level humidity (Simpson et al., 2023), we do not consider model projections of humidity. Instead, in Figure 10 we show near future change in precipitation, SST and 700 hPa heights for all seasons. To look at the future we examine the next two-decade period (2031–2050) relative to the last two decades (2001–2020). This is particularly important for the Southern Hemisphere given the decline of ozone until about 2000 and then its subsequent stabilization and gradual recovery (Solomon et al., 2016). Looking at differences relative to a late 20th century baseline would include the consequences of ozone depletion (as in figures already shown) but what is of interest is how hydroclimate will change now that ozone is recovering gradually but GHGs are continuing to rise. In

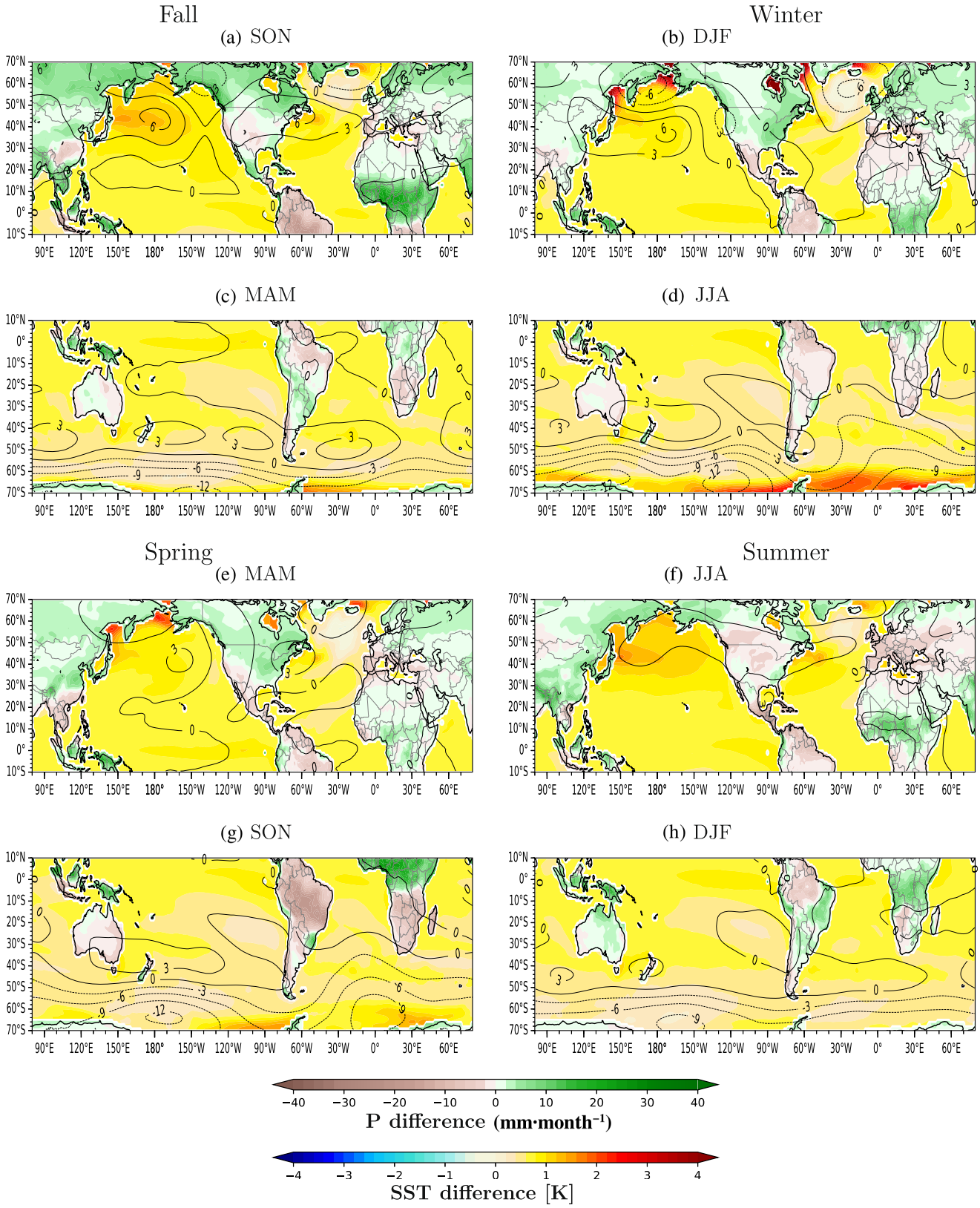

FIGURE 10 Legend on next page.

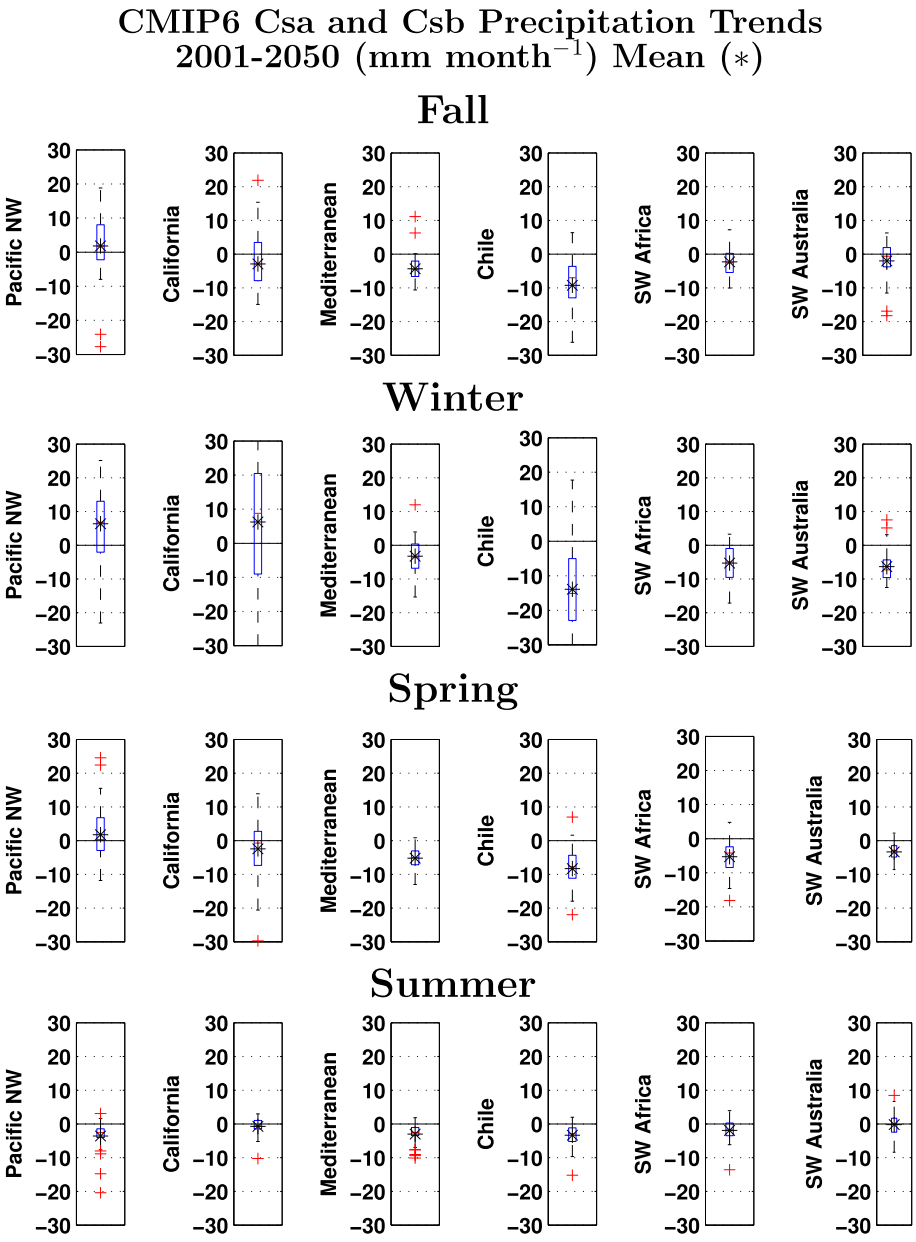

FIGURE 11 Model projections of precipitation trends from 2001 to 2050 for the world's MCRs and for, from top to bottom, fall, winter, spring and summer. The multimodel ensemble mean is marked by an asterisk. The edges of the box mark the 25th and 75th percentile of the ensemble spread across model ensemble means, the horizontal line is the median, the whiskers mark the range and outliers (beyond one and a half times the inter-quartile range from the 25th or 75th percentiles) are red crosses. Units are for the change over 2001–2050 expressed in mm·month^{-1}.

the Southern Hemisphere, the future circulation differences are very similar to the trends seen to date but weaker: increased geopotential heights in the mid-latitudes and decreased heights further poleward throughout the year. This goes along, as it did for the last few decades, with drying in all the Southern Hemisphere MCRs in all seasons. At least in these model projections and for this time frame it appears the drying influence on MCR hydroclimate of rising GHGs wins out over any wetting influence from ozone recovery.

In the Northern Hemisphere matters are once again more complicated. In winter, the models project higher heights over the central North Pacific and a trough at the west coast of North America and then a ridge over the central Mediterranean. Consistently there is wetting over the North American MCR north of southern California and drying across the Mediterranean. In spring the Mediterranean ridge remains, though weaker, but the trough over the North American west coast has gone and the MCR dries south of Washington State. Summer has

FIGURE 10 CMIP6 multimodel mean projections of SST (colours, ocean), 700 hPa heights (contours) and precipitation (colours, land) for (a, c) fall, (b, d) winter, (e, g) spring and (f, h) summer. Projections are for a near-term future (2031–2050) minus a recent past (2001–2020). Units are K for SST, m for heights and mm·month^{-1} for precipitation.

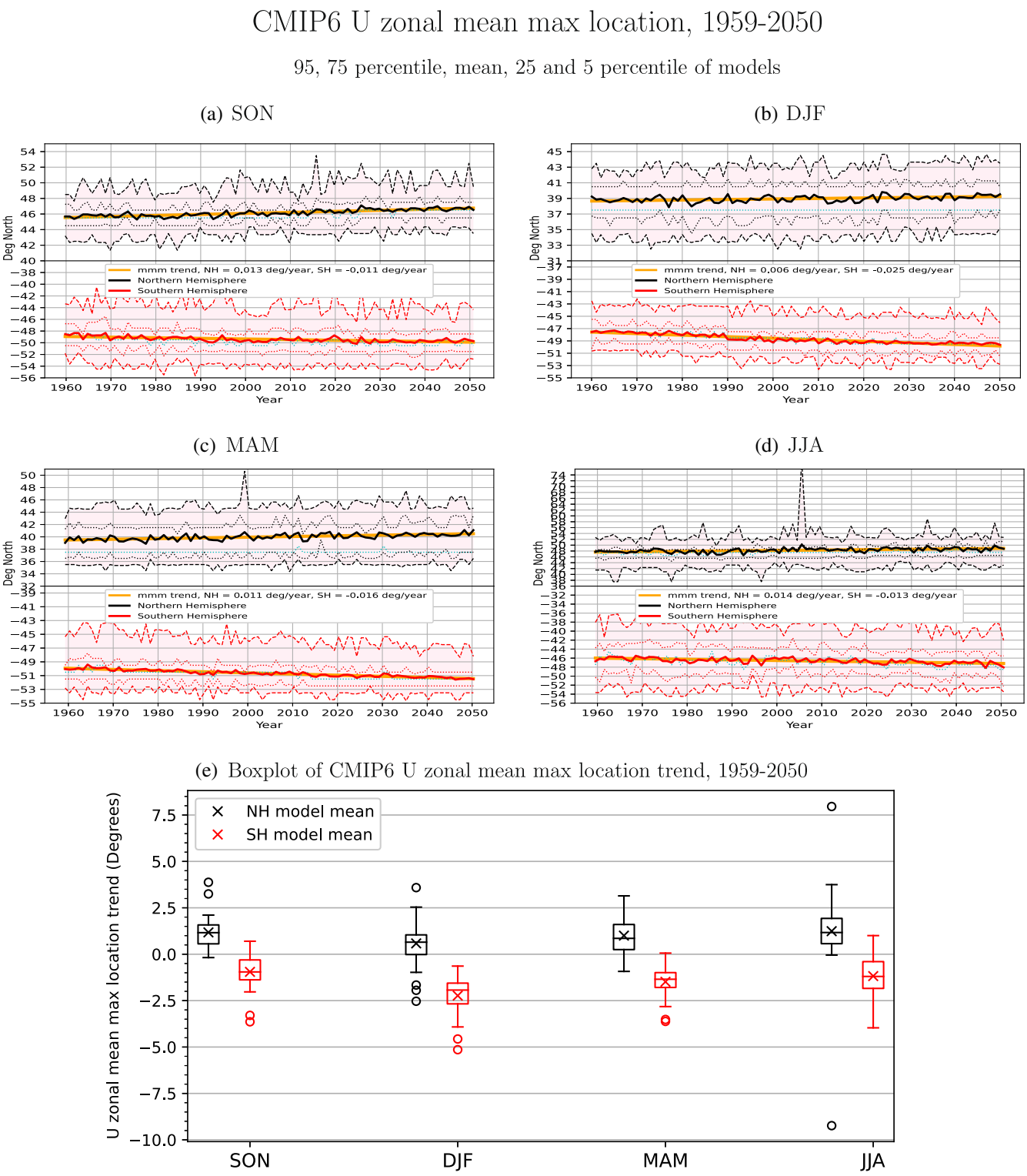

FIGURE 12 Model projections of the latitude of maximum zonal mean zonal wind at 700 hPa from CMIP6 historical and future projections. The mean across models of the ensemble mean for each model is shown as the solid line and the dashed lines show the 25/75th and 5/95th percentiles of the distribution across models and ensemble members. The linear least squares trend lines are also shown with their gradients noted. Units are degrees latitude. In the lower panel the ensemble spread across models and runs of changes in latitude over the time period is shown in box and whiskers format. The edges of the boxes show the 25th and 75th percentile spread and the whiskers extend from the box to the farthest data point lying within 1.5 times the inter-quartile range from the edges of the box, with outliers beyond marked. The line across the box is the ensemble median and the cross is the mean.

strong drying over the Mediterranean that does not seem associated with any similarly strong circulation anomaly and there is also drying along the North American coastal MCR. Both Northern Hemisphere MCRs are projected to dry in fall.

Model-projected trends over 2001 to 2050 are shown in box and whiskers format in Figure 11. With robustness indicated by when more than 75% of models agree on sign of change, the results indicate robust drying trends in all the Southern Hemisphere MCRs and in all seasons except southwest Australia in summer and fall. Robust drying in the Mediterranean in all seasons and in the Pacific Northwest in summer is projected by CMIP6. There are no robust projected wetting trends but there are suggestions (i.e., a majority of models) of a wet trend in the whole North American MCR in winter.

Further context for projected climate change and the contrast between hemispheres is provided in Figure 12 which shows the latitude of maximum zonal mean zonal wind at 700 hPa (the eddy-driven jet, see Simpson et al., 2014) for 1959–2050 in the historical and future projection simulations of CMIP6. Summer (DJF) in the Southern Hemisphere shows a poleward shift of the jet during the period of ozone depletion up to about 2000 but then continues more weakly to 2050. Southern Hemisphere spring, fall and winter show poleward shifts across historical and future periods. In the Northern Hemisphere, poleward shifts of the jet occur in fall, spring and summer. The opposite signed responses between the North Pacific and Atlantic sectors in DJF prevents any strong zonal mean response, as shown by Simpson et al. (2014). Robustness and significance are further assessed in Figure 12e using box and whiskers plots of the ensemble spread across models and runs of the latitude shift over the period. Robustness, as in more than 75% of runs agree on the sign of change, is evident for the shifts mentioned above. The box and whiskers clearly show the widening of the tropics-to-subtropics band between the jets but also makes clear that the shift is larger and more robust in the Southern Hemisphere. At least for the Southern Hemisphere MCRs, these results emphasize the likelihood of continuing aridification associated with poleward shifts of the jets driven by rising GHGs.

5 | ROBUSTNESS OF PRECIPITATION CHANGE OVER THE 21ST CENTURY WITHIN MULTIPLE LARGE ENSEMBLES

Here we make use of the 10 large ensembles to examine the uncertainty in model projections of precipitation in the MCRs and see the relative contributions from model response differences and internal model variability. Figure 13 shows time series of 20-year running mean annual (for brevity) precipitation from 1980 to 2100, a longer period than analysed so far but one that places the ongoing and near-term future changes in context. Also shown are the observational estimates from CRU and GPCC. For the historical period the observational estimates fit within the model spread with the exception of CRU for southwestern South Africa which has considerably greater variability and a stronger drying trend (as also seen in Figure 3). Looking forward, what is once more remarkable is the extent of model agreement that the Southern Hemisphere MCRs will continue to dry. For Chile and southwest Africa, by 2050 there is almost no uncertainty as to the sign of annual mean precipitation change: the vast majority of models and ensemble members predict drying. This level of agreement is delayed until 2070 for southwest Australia. As a group, the models all predict intensifying drying of southern MCRs for the entire century. However, the spread due to model differences and internal variability is such that the drying could range between about 50% and 150% of the mean drying. For Chile and southwest Africa, uncertainty from model differences is a bit larger than from internal variability while for southwest Australia uncertainty is about equally divided. Models also agree on drying in the Mediterranean. However, in this case, the modelled best case delays drying until the early second half of the century and with 0.2 $mm \cdot day^{-1}$ by end of the century. In contrast, in the worst-case scenario, that amount of eventual drying has already occurred and will intensify to three times as severe at about 0.6 $mm \cdot day^{-1}$. In the Mediterranean region, model differences are the larger contributor to uncertainty. Results are starkly different in the North American MCR. The large ensembles project modest forced drying in California has already occurred with no further change and wetting in the Pacific Northwest but the spread contains wetter and drier futures for both regions. Also, in both parts of the North American MCR, the uncertainty mostly arises from internal variability for the first half of this century, but by the end of the century there are about equal contributions from differences between models and from internal variability.

6 | DISCUSSION

6.1 | Observed and modelled trends to date

The trends in precipitation, surface and low-level humidity and VPD in the Southern Hemisphere over the past five decades appear well related to the trends in zonal

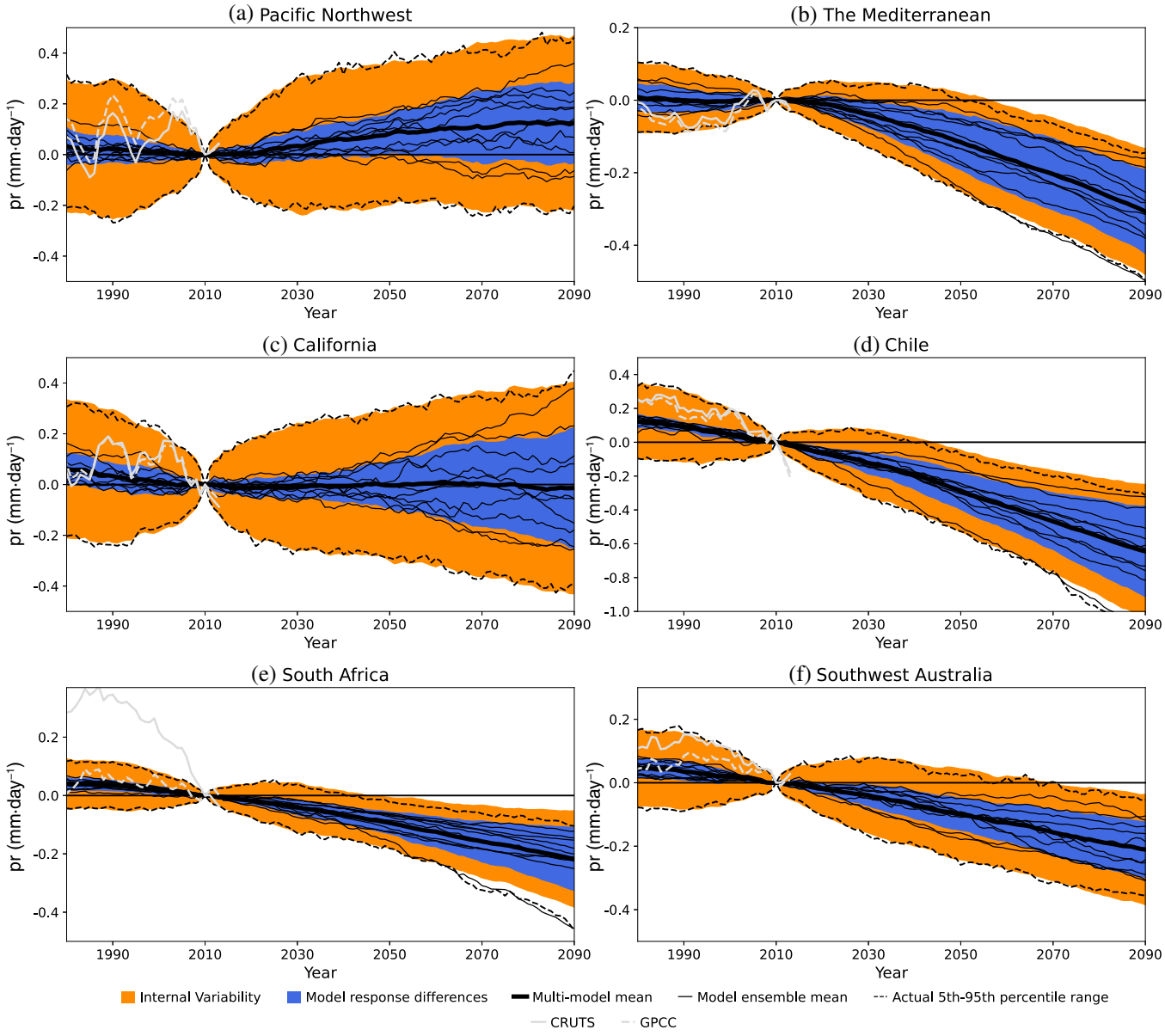

FIGURE 13 20-year running annual mean precipitation anomalies, relative to 2001–2020, for 10 large ensembles consisting of 20 members each. Thin dark lines show the ensemble means for each individual model and the thick black line shows the multi-model ensemble mean. The edge of the orange shading shows the 90% confidence interval across the ensemble members and this is partitioned into a contribution due to model response differences (blue) and internal variability (orange) following the method of Hawkins and Sutton (2009) and Lehner et al. (2020). The dashed black lines the 5th to 95th percentile range of the distribution of the model members. Also shown are the corresponding values from the observational CRU and GPCC data. Units are mm·day^{-1}.

mean winds, eddy momentum fluxes and subsidence. Of great importance for hydroclimate and its impacts on MCRs, these circulation-driven precipitation drying trends appear in all seasons. This across-seasons climate change is consistent with simulations of climate models driven by changes in radiative forcing. It is proposed that it arises as a result of both increases in GHGs and depletion of ozone. The latter only directly impacts climate in the summer half year when ozone can interact with incoming solar radiation. Considerable work has attributed a poleward shift of the jet, Hadley cell and subtropical dry zone expansion in austral summer to ozone depletion (e.g., McLandress et al., 2011; Polvani et al., 2011; Thompson et al., 2011). The time evolution of this is a strong shift as ozone depleted in the late 20th century and then stabilized following international action initiated by the Montreal Protocol (see Banerjee et al., 2020). Over our time period, this still appears as a

poleward trend. In the austral winter half-year the same direction trend arises from rising GHGs and can involve some of the same stratosphere-troposphere dynamical interaction mechanisms that drive the response to ozone. Our results are consistent with those of Fogt and Marshall (2020) who show trends towards a poleward-shifted and stronger Southern Annular Mode in all seasons over the past half-century. As here, these are strongest in austral summer but, in their work, still can reach statistical significance in austral winter. Grise et al. (2019) report consistency between models and observations in the expansion of the Southern Hemisphere Hadley Cell with both GHGs and ozone depletion contributing. Here we argue that these human-driven changes are causing reductions in precipitation in the three Southern Hemisphere MCRs and increases in surface and low-level atmospheric aridity west of and over the Chile and southwest Africa MCRs.

The Northern Hemisphere is far more complicated with changes in precipitation in North America and the Mediterranean being different and both varying by season. This is no doubt due to the higher amplitude stationary wave field playing a role, the weaker ozone forcing, the strength of the influence of the tropical Pacific on North America and the presence of localized modes of atmosphere variability such as the North Atlantic Oscillation (NAO). In North America there has been reducing precipitation in fall from Oregon south with wetting in Washington, a north–south drying–wetting dipole in winter, mostly wetting apart from southern California in spring and drying along the coast in summer. Of these only the all-coast precipitation reduction in summer and the drying in fall from Oregon south agree with CMIP6 simulations of the response to radiative forcing. The fall precipitation reduction was noted by Lukovic et al. (2021) and is consistent with a later onset, shorter, rain/snow season (e.g., Swain, 2021). However, the CAM6 model forced by both the observed SST history and trace gases does not reproduce the spring and fall trends in precipitation in the North American MCR and associated circulation. This suggests, albeit based on just one SST-forced model, the observed trends might in fact be strongly influenced by internal atmosphere variability and any agreement of them with the CMIP6 models is fortuitous. Prior work on November–April precipitation trends in California has also not found evidence of drying or wetting (Seager et al., 2015). This stands in contrast to a drying trend in spring in the interior southwest that is apparent in observations, CMIP6 radiatively-forced models and SST-forced models (Seager et al., 2022b).

In contrast to the North American MCR, there has been reduced precipitation in the Mediterranean region since 1959. This drying stretches across almost the entire Mediterranean in winter and is also widespread though weaker in spring. S19 showed notable agreement between the observed and CMIP6 modelled drying in the Mediterranean in winter for the period 1901–2018. Here we show the observed drying in spring and northwest Africa and parts of the Middle East are also seen in CMIP6 simulations of radiatively-forced change. Earlier work that examined the entire cool, wet half of the year (November–April) claimed that there was a combined model and observations-based evidence of human-driven precipitation decline across the Mediterranean as a consequence of human-driven ocean warming (Hoerling et al., 2014). Looking at 1950–2004 and the entire wet season, Kelley et al. (2012) found evidence of human-driven drying once the effects of presumed natural decadal fluctuations of the NAO had been removed. However, in our updated analysis, the observed drying in spring appears related to a low-level high anomaly over western Europe and low over Russia that brings drying continental air to the central and eastern Mediterranean and sub-Saharan air to the western Mediterranean. This circulation trend is not seen in either the CMIP6 models nor the SST-forced model. This discrepancy cautions that there are likely seasonal variations in the mechanisms of Mediterranean drying and we should not yet draw a firm conclusion on the role of human-induced climate change in spring precipitation trends in the Mediterranean. This conclusion also holds for the winter and summer season changes not shown here.

6.2 | Modelled near-term future trends in seasonal precipitation

The near-term future trends, evaluated from 2001 to 2050, in CMIP6 models essentially continue the simulated trends to date. All the Southern Hemisphere MCRs continue to dry in all seasons, indicating that the effect of GHG-induced warming wins out over any wetting due to ozone recovery. In the Northern Hemisphere the models project Mediterranean drying throughout the year. In the North American MCR the models project drying in the fall in the south, wetting in winter, drying in the south and wetting in the far north in spring, and drying in summer. The future drying trends across-seasons are quite robust across models and ensemble members in the Mediterranean, Chile and southwest Africa and in Australia in winter and spring. In contrast, the trends in the North American MCR are less robust, with models suggesting either a drying or wetting is possible, except for drying in the Pacific Northwest in summer. According to the Large Ensembles, the drying is robust in all southern MCRs and the Mediterranean, although with timing and

magnitude influenced by model response uncertainty and internal variability uncertainty, but not at all robust in the North American MCR. Within the large Mediterranean MCR, all grid points in the current Csa and Csb areas have drying trends in spring and summer, 98% in fall and 86% in winter, emphasizing that this is a regional-scale climate change. Previously, Polade et al. (2017) reported using CMIP5 models the projected winter drying of all the MCRs other than California which agrees with that part of our analysis.

6.3 | Physical mechanisms of observed humidity changes and observed and modelled future precipitation trends

6.3.1 | The Southern Hemisphere

The causes of changes to date in precipitation and humidity in the Southern Hemisphere MCRs at least appear relatively straightforward. The greater degree of zonal symmetry in the Southern Hemisphere essentially ensures that the MCRs tend to change together in response to radiative forcings from ozone and rising GHGs that themselves are largely zonally symmetric. In spring to summer, ozone depletion impacts stratospheric temperatures and flow. Changes in lower stratosphere flow can influence the fluxes of momentum by synoptic eddies in the upper troposphere which then change the mean meridional circulation throughout the depth of the troposphere (see, e.g., Thompson et al., 2011, and references therein). Rising GHGs can also shift the mid-latitude jet streams poleward (Grise & Polvani, 2011) via mechanisms involving stratospheric temperature and circulation change akin to those for ozone depletion (e.g., Wu et al., 2012, 2013a, 2013b; see Shaw, 2019 for a comprehensive review of mechanisms originating in the stratosphere, troposphere and surface). Hadley Cell expansion can also follow directly from radiative effects of increasing CO_2 without changes in surface temperature (Lu et al., 2008). However, general warming of the surface due to rising GHGs also achieves a similar zonal mean circulation response (e.g., Frierson et al., 2007) and dries the Southern Hemisphere MCRs (Garfinkel et al., 2020). Unlike ozone depletion, the direct and indirect effect of rising GHGs work year-round. Hence these two radiative forcings, via multiple mechanisms, are capable of explaining the poleward-shifted westerlies.

S19 used a moisture budget decomposition to explain future drying of the Southern Hemisphere MCRs in winter in terms of reduced mean circulation moisture convergence. The circulation change was towards easterly anomalies and enhanced subsidence, both of which would be expected to induce drying. The commonality of circulation changes across seasons seen in Figure 10 suggests these mechanisms of drying likely play a role throughout the year.

6.3.2 | The Northern Hemisphere

In the Northern Hemisphere the mechanisms are different and the poleward shift of the jets is less obvious. Watt-Meyer et al. (2019) have shown this is partly related to, first, the spatial patterns of CO_2-induced SST change which impart greater static stability changes in the southern than Northern Hemisphere and, second, the Hadley Cell width being less sensitive to static stability changes in the northern than Southern Hemisphere. In addition, the Northern Hemisphere introduces more zonal asymmetry such that the two MCRs have responded, and are projected to continue to respond, differently to drivers of climate variability and change. This is related to the stronger stationary wave field in the Northern Hemisphere, with its stark land-ocean thermal contrasts throughout the year and high mountains in North America, Asia and the Mediterranean basin. In response to these asymmetries there are distinct extratropical jet streams and storm tracks over the Pacific and Atlantic Oceans (Hoskins & Valdes, 1990). Further, Arctic amplification of warming, for which there is no Southern Hemisphere counterpart, drives a reduction in the low-level meridional temperature gradient that opposes the upper level increase caused by the combined effects of upper troposphere warming and tropopause rise in the Tropics and extratropical stratospheric cooling (e.g., Chen et al., 2020). This might weaken zonally symmetric responses to forcing while increasing the relative importance of stationary wave responses. Considering the radiatively-forced change first, Grise and Polvani (2011) show that, despite the zonal asymmetries of the mean Northern Hemisphere climate, the response to rising CO_2 in the absence of SST change induces a poleward shift of the jets over both oceans in all seasons and a high-pressure anomaly over the Mediterranean in winter and spring (consistent with drying). But they also show that the response to the SST changes induced by the rising CO_2 is zonally asymmetric, enhancing the poleward jet shift over the North Atlantic-Europe-Mediterranean region, but inducing an equatorward shift over the eastern Pacific and west coast of North America. This shift is strongest in the winter and the associated SST-induced ridge over the Mediterranean and trough over the North American west coast is consistent with model projections of drying in the Mediterranean but wetting in the North American MCR. An interesting aspect of this is that

Simpson et al. (2016) showed that the wetting–drying North America–Mediterranean contrast can be explained in terms of the intermediate scale stationary wave response to the zonal mean zonal wind change in the subtropics to mid-latitudes. Hence, to be consistent with Grise and Polvani (2011), requires that the CO_2-induced SST change, with all its spatial structure, drives the right zonal mean wind change in the subtropical to mid-latitudes upper troposphere that influences the propagation of stationary waves. This is entirely possible because an important signal of CO_2-induced SST change in both models and observations is a warming over the regions of deep convection which would lead to a relatively uniform warming of the tropical upper troposphere through moist adiabatic adjustment and a strengthening of the westerlies in the subtropics.

The model simulated and projected response to GHG forcing in the Mediterranean is largely consistent with the observed record of winter and spring drying to date. However, in the North American MCR the record is varied with only spring in California showing a weak radiatively-forced-model simulated drying and even that being inconsistent with observations. However, these agreements, such as they are, are potentially fortuitous. In no season do the observed circulations trends that drive the observed precipitation trends look like those in the radiatively-forced multimodel mean. The starkest difference (not shown here) is the wintertime strengthening of the North Atlantic jet and high pressure anomaly over the Mediterranean which is not even approximately reproduced in the radiatively-forced multimodel mean, as pointed out by Blackport and Fyfe (2022). The disagreements in circulation trends over the North Pacific and west coast of North America between observations and the radiatively-forced models are also obvious. Further, in no season are there agreements across the observations, SST-forced model (albeit a single model) and CMIP6 models on circulation trends. This suggests that the disagreements between observations and radiatively-forced models do not come about from strong naturally occurring SST variations (as Blackport and Fyfe also concluded). Mediterranean precipitation variability is highly influenced by the NAO and, to a lesser extent, by other modes of atmospheric variability and does not appear to be strongly ocean-driven (see S19 and references therein). Precipitation variability in California and along the North American west coast does have a relation to tropical Pacific SST variability but even this is weaker than that due to internal atmosphere variability (Seager et al., 2015). Hence for both Northern Hemisphere MCRs it is not unreasonable to think that even long-term trends might arise from internal atmosphere variability. But clearly, with this level of disagreement amongst models and observations, no firm conclusions can be drawn.

Turning to the changes in surface and low-level humidity, it is notable that the Northern Hemisphere does not have analogs to the longitudinally widespread, low-level atmospheric drying seen in the Southern Hemisphere subtropics to mid-latitudes. There are regions of drying under subsidence in the central subtropical North Pacific and Atlantic Oceans but these are considerably equatorward of the MCRs. However, there actually is a region of surface and low-level humidity decrease over southern California and the interior southwest United States in spring. Jacobson et al. (2023) confirmed this atmospheric drying in in situ station data, and have attributed it to less evapotranspiration into the atmosphere following a strong March trend towards less precipitation. There are also regions in the Mediterranean—for example, Iberia, Morocco and Turkey—that are experiencing surface and low-level humidity declines or little increase. This is surprising since our default expectation is for an increase following Clausius-Clapeyron with warming even if relative humidity declines over land (Byrne & O'Gorman, 2016). This atmospheric drying, together with that occurring in many semi-arid and arid regions of the world, is the focus of the analysis of Simpson et al. (2023) who show that state-of-the-art climate models conspicuously fail to simulate it. Their study focuses on land areas and suggests that the most likely candidate for the discrepancy between models and observations may arise from incorrect land–atmosphere interactions in models. Here we show that atmospheric drying also occurs over some subtropical to mid-latitude oceans. In this case moisture budget analyses of ERA5 data (not shown here) indicate it is induced by mean circulation anomalies and (also not shown) is not well reproduced in CMIP6 simulations of the historical period.

Considering the near-term future projections in the Northern Hemisphere, the models project reduced precipitation across most of the Mediterranean throughout the year. In contrast, the models project most of the North American MCR to get wetter in winter but drier in the rest of the year consistent with Dong et al. (2019). Simpson et al. (2016) argued that changes in the intermediate-scale stationary wave field following strengthening of the subtropical upper troposphere jet could help explain this zonal asymmetry of changes in northern MCR climates, while also showing that larger-scale waves contribute to Mediterranean drying. The role of stationary wave changes is made more complex by claims, building off interannual variability relations, that models might underestimate the Mediterranean winter precipitation decline for a given stationary wave change

(Zappa et al., 2015b) while Tuel et al. (2021) argue the opposite based on models underestimating the mean state vertical wind shear over the eastern Mediterranean. In addition, models tend to project that the eastern tropical Pacific will warm more than the rest of the tropical Pacific (often called an El Niño-like response) and Allen and Luptowitz (2017), Dong and Leung (2021) and Seager et al. (2023) have pointed out this model response to rising GHGs tends to make California wetter in winter. However, it is now widely accepted that there is a discrepancy between the observed trend to an enhanced zonal SST gradient across the equatorial Pacific and model simulations of the historical period (Lee et al., 2022; Olonscheck et al., 2020; Seager et al., 2019a, 2022a; Watanabe et al., 2020) indicating future projections should be treated with caution. Hence the model projections of mid-winter wetting of California should be treated with caution. The spring drying along the North American west coast may be more certain. Ting et al. (2018) explain this in terms of enhanced advective drying by the mean westerlies as spring warming over land increases atmospheric humidity such that the zonal humidity gradient (wetting to the east) strengthens. This thermodynamic effect is likely less influenced by the structural uncertainty of models than the dynamical effects at play in the winter (e.g., Shepherd, 2014). Notably, the North American MCR is the one where internal variability introduces the greatest fractional uncertainty to future precipitation projections. Add to this the discrepancy between modelled and observed humidity trends in this region (Simpson et al., 2023) then it is clear that the hydroclimate future of the North American MCR is uncertain.

In addition to changes to global stationary waves as in Zappa et al. (2015b) and Simpson et al. (2016), other mechanisms have been identified to help explain why the Mediterranean is such a hotspot of drying, year-round, in both the past and the future. Tuel and Eltahir (2020) and Tuel et al. (2021) recognize the importance of the planetary scale stationary waves but also show that greater GHG-induced warming over land than the Mediterranean Sea in winter leads to a localized high over the Sea that suppresses precipitation. During the winter much precipitation is associated with the Mediterranean storm track (Lionello et al., 2006). Indeed, Seager et al. (2014) found that in CMIP5 models there was enhanced transient eddy moisture flux in the cool season onto the land areas north of the Sea which followed from enhanced moisture gradients. This partially offset the mean-flow induced drying. On the other hand, Zappa et al. (2015a) found that the winter precipitation reduction is associated with a reduced number of cyclones even as locally, cyclone-associated precipitation can increase. Given the technicalities of moisture budget evaluations and cyclone-tracking and precipitation tagging these results are not necessarily at odds with one another.

Another possible driver of cool season Mediterranean drying is the behaviour of the subpolar North Atlantic Ocean. Delworth et al. (2022) show that in a 21st century model scenario where GHGs are reduced, the North Atlantic becomes relatively cool because the Atlantic Meridional Overturning Circulation, which weakened over the late 20th to middle 21st century, does not recover. In winter the cool subpolar North Atlantic SSTs lead to a cyclone above and a teleconnected anticyclone, inducing drying, over the Mediterranean. While focused on a model future, this work suggests that the North Atlantic warming hole and its continuation into the future could be contributing to cool season Mediterranean drying. Notably, in the future winter model projections shown here, the North Atlantic cyclone-Mediterranean anticyclone and cool North Atlantic SSTs appealed to by Delworth et al. are also seen (Figure 10) although, independently, the acceleration of the upper tropospheric, subtropical, zonal mean zonal flow can also induce a high over the Mediterranean (Simpson et al., 2016). Of course, the Mediterranean might be such a hotspot for drying exactly because multiple mechanisms are inducing drying in that region and acting additively.

The Mediterranean is also projected to dry in the warm season. Seager et al. (2014) used a moisture budget decomposition on CMIP5 models to attribute this to anomalous mean flow moisture divergence with both enhanced moisture and enhanced mass divergence contributing. The increased heights over the North Atlantic Ocean shown here (Figure 10), and equatorward flow over the Mediterranean longitudes, are consistent with those arguments. The high-pressure ridge extends from the western North Pacific to the Atlantic and could also help explain the summer drying over the northern reaches of the North American MCR. Tuel and Eltahir (2021) argue that cool season precipitation reductions can set the stage for summer drying via soil moisture-precipitation feedbacks with the associated low-level anticyclone over Europe displacing Atlantic moisture inflow northward and away from the Mediterranean.

6.4 | Future shifts of the locations of MCRs

We have considered past and projected future climate change within the current geographic locations of Csa and Csb (Mediterranean) climate zones. However, the changes projected imply that the MCRs will move.

TABLE 1 Agreement on sign of precipitation trends for MCRs by season, 1959–2021 and for model projections of 2001–2050.

	PNW	CA	Med	Chile	SW Africa	SW Australia
Fall	R_P	O*+, R_P	S, $\mathbf{R}_F$	O, R_P, S, $\mathbf{R}_F$	O, R_P	O
Winter	O, S	S	O*+	O, R_P, S, $\mathbf{R}_F$	S, $\mathbf{R}_F$	O*, R_P, *S*, $\mathbf{R}_F$
Spring		*O**, S	O, $\mathbf{R}_F$	O, R_P, S, $\mathbf{R}_F$	$\mathbf{R}_F$	R_P, $\mathbf{R}_F$
Summer	O*, R_P, $\mathbf{R}_F$	O*	O*, R_P, $\mathbf{R}_F$	O*, R_P, S, $\mathbf{R}_F$		

Note: Observed agreement is when both or all three (North America only) observational data sets agree on sign of trend. For the models agreement is when three quarters or more of the model ensemble means for CMIP6, and the model ensemble members for CAM6, agree on sign of trend. All but two trends are drying with the wetting trends (observed CA, spring and SST-forced Southwest Australia, winter) in italics and underlined. Future trends are in bold face. If the observed trends do not overlap with the 5th to 95th percentiles of the SST-forced ensemble members or the CMIP6 ensemble means they are marked with asterisk and/or plus signs, respectively.
Abbreviations: O, observed; R_P, radiatively-forced CMIP6 for past; S, SST-forced CAM6; R_F, radiatively-forced CMIP6 for future.

Alessandri et al. (2014) used CMIP5 climate projections to probabilistically project the future location of MCRs. They found that warming and increased seasonality of precipitation caused the North American and Mediterranean MCRs to expand northward and eastward. They also found that decreasing cool season precipitation shifted the climate in the southern coastal United States, northwest Mexico, northwest Africa and the northern shores of the Mediterranean Sea from MCR to arid. This is consistent with our findings for the Mediterranean but the uncertainty of changes in precipitation for the California-Mexico region, including the possibility of more winter precipitation, counsels caution there. In the Southern Hemisphere the projected precipitation decline and poleward jet stream movement diagnosed here are consistent with the reduction in areas of MCRs in southwestern Africa and southwest Australia as the climate conditions needed for an MCR shift southward of the continents. In Chile we would expect a southward shift of the MCR but that requires further examination as it is not what was found in Alessandri et al. (2014).

7 | CONCLUSIONS

Changes in important aspects of hydroclimate—precipitation, vapour pressure deficit and specific humidity—have been examined across seasons for the worlds five Mediterranean climate regions. VPD, and its contributing factors of temperature and specific humidity, were examined because of the tight influence this has on burned forest area at least in North America and likely in other MCRs too. Changes over 1959–2021 have been placed in the context of large-scale changes in circulation. We then examined model projections of future changes in precipitation. Table 1 provides a summary of findings and presents a simple assessment of observed and model agreement on the sign of trends for all MCRs by season for the historical period and for the 2001–2050 projected future. It is striking that across observations, modelling frameworks, time periods and seasons, only two of these agreed upon trends are wetting. The table makes clear the widespread agreement on: past and future drying in Chile; future spring drying in MCRs other than in North America; winter drying in the Southern Hemisphere MCRs. The table also emphasizes the observed summer drying in North America, the Mediterranean and Chile, which in all cases is not captured by the SST-forced ensemble but is by the CMIP6 ensemble. In addition observed winter drying in California and the Mediterranean is beyond the range of both ensembles while spring wetting in California is beyond the SST-forced ensemble. More detailed conclusions are as follows:

1. Qualitative attribution of precipitation trends to date to radiative forcing is judged to occur when different observational data sets and 75% or more of CMIP6 model ensemble means agree on the sign of the change. By this standard, radiatively-forced drying is occurring in the Chilean MCR in all seasons, in southwestern Africa in fall, southwest Australia in fall and winter, California in fall and the Pacific Northwest in summer. In no MCR in any season is there evidence of radiatively-driven wetting. Whether fall drying in the North American MCR can really be attributed to radiative forcing is however brought into question because an atmosphere model forced by the observed SST history produces a North Pacific-North American circulation trend at odds with that observed or in the CMIP6 models. Why there is apparently more agreement between observations and CMIP6 models on precipitation change than on circulation requires further investigation and explanation.
2. Vapour pressure deficit (VPD) in spring in the ERA5 reanalysis has increased as expected given the control of warming temperatures on the saturation humidity. More surprising is that the specific humidity has either not increased or actually declined in

southwestern North America including the California MCR, and, more starkly, across the Southern Hemisphere subtropical to mid-latitude oceans west of the MCRs.

3. The precipitation reduction and atmospheric drying in the Southern Hemisphere can be dynamically related to a change in the mean meridional circulation with a poleward shift of the jet, enhanced poleward transient eddy momentum flux and eddy-driven subsidence at the latitude of the MCRs. These changes are consistent with the expectations of the response to a combination of ozone depletion and GHG increase as demonstrated in numerous other observational and modelling studies.
4. CMIP6 model-based trends from 2001 to 2050 show striking reductions in precipitation in the Mediterranean in all seasons and in all the Southern Hemisphere MCRs in all seasons other than summer and fall in southwest Australia. This period covers the one of expected ozone recovery and, hence, for the Southern Hemisphere, reveals the dominance on near-term future MCRs hydroclimate of CO_2 rise over ozone recovery and continued drying. Dynamically continued drying appears related to further intensification and poleward shift of the Southern Hemisphere jet with easterly anomalies and subsidence at the MCRs latitudes. In the North American MCR projected future trends are not clearly distinct from zero with the qualified exception of wetting in the Pacific Northwest in winter and drying in summer.
5. The uncertainty introduced into model projections by model responses to forcing and internal variability was examined using 10 large ensembles. This shows that ongoing drying of Southern Hemisphere MCRs is remarkably robust, though with variations in magnitude and timing across models. Drying of the Mediterranean is also robust but with its timing ranging from already ongoing to becoming discernible in mid-century with this range strongly influenced by model-based uncertainty. Projections are uncertain for the North America MCR largely due to model-based uncertainty.

These results, drawn from observations and climate models, present a concerning picture of hydroclimate in the MCRs. The Southern Hemisphere MCRs will face increasingly challenging conditions in terms of water resources as the subtropics expand and the extratropical jets migrate southward away from the MCR locales. The Mediterranean region will also face further drying while the North American MCR might actually become wetter in mid-winter but drier in other seasons. It has been argued that these changes represent a poleward movement and expansion, in the Northern Hemisphere, of Mediterranean-type climates (Alessandri et al., 2014). The dynamical changes underlying the drying of the southern MCRs are reasonably certain but what stationary wave and local processes are driving the Mediterranean drying and the contrasting conditions in North America, remains unclear. Notably, predictions of winter wetting of California might not be correct. If the eastern equatorial Pacific continues to not warm, in contrast to model projections, then this could induce a drying tendency for California but a wetting tendency for the Pacific Northwest. Further dynamically-focused attribution work is needed to determine the causes of observed trends being beyond the range of model ensembles (the Mediterranean in winter and California in fall) and why the SST-forced ensemble cannot simulate observed summer drying in American and European MCRs. Expanding the number of SST-forced ensembles, if possible, would be a priority. On top of these concerns is uncertainty as to how VPD will evolve. As presented here there is evidence VPD increases in or near many MCRs is being contributed to by a lack of increase or even a decrease in actual vapour pressure. Given model inability to simulate these trends (Simpson et al., 2023), it is hard to project these changes forward but should they continue they will add to the precipitation changes reported here to further increase fire hazard. Clearly all the MCRs are facing serious climate change-induced stresses in the coming decades that need to be planned for now.

AUTHOR CONTRIBUTIONS

Richard Seager: Conceptualization; investigation; funding acquisition; writing – original draft; methodology; validation; visualization; formal analysis; project administration. **Yutian Wu:** Conceptualization; investigation; funding acquisition; methodology; validation; writing – review and editing; formal analysis. **Annalisa Cherchi:** Conceptualization; investigation; funding acquisition; methodology; validation; writing – review and editing; formal analysis. **Isla R. Simpson:** Conceptualization; investigation; methodology; validation; writing – review and editing; formal analysis. **Timothy J. Osborn:** Conceptualization; investigation; methodology; validation; writing – review and editing; formal analysis. **Yochanan Kushnir:** Conceptualization; investigation; funding acquisition; methodology; validation; writing – review and editing; formal analysis. **Jelena Lukovic:** Writing – review and editing; investigation; methodology; validation; formal analysis. **Haibo Liu:** Investigation; methodology; validation; visualization; writing – review and editing; formal analysis; data curation; software. **Jennifer Nakamura:** Investigation;

writing – review and editing; visualization; validation; methodology; formal analysis; software; data curation.

ACKNOWLEDGEMENTS

RS, YW and YK were supported by NSF award AGS-2127684. IRS acknowledges support from the NSF National Center for Atmospheric Research, which is a major facility sponsored by the National Science Foundation under the Cooperative Agreement 1852977. AC acknowledges support from the OptimESM project, European Union's Horizon Europe Research and Innovation Programme under GA number 101081193. An early version of this work was presented in September 2022 at MedCLIVAR in Marrakesh, Morocco for which we thank the conference organizers and the hospitality of faculty, staff and students at Université Cadi Ayyad, Marrakesh. We thanks two anonymous reviewers for useful critiques.

CONFLICT OF INTEREST STATEMENT

The authors declare no conflicts of interest.

DATA AVAILABILITY STATEMENT

The data that support the findings of this study are available from the corresponding author upon reasonable request.

ORCID

Richard Seager https://orcid.org/0000-0003-4772-9707
Yutian Wu https://orcid.org/0000-0002-4428-6624
Annalisa Cherchi https://orcid.org/0000-0002-0178-9264
Isla R. Simpson https://orcid.org/0000-0002-2915-1377
Timothy J. Osborn https://orcid.org/0000-0001-8425-6799
Yochanan Kushnir https://orcid.org/0000-0003-3312-5160
Jelena Lukovic https://orcid.org/0000-0001-8967-3495
Haibo Liu https://orcid.org/0000-0002-8555-8569
Jennifer Nakamura https://orcid.org/0000-0003-4113-8519

REFERENCES

Alessandri, A., De Felice, M., Zeng, N., Mariotti, A., Pan, Y., Cherchi, A. et al. (2014) Robust assessment of the expansion and retreat of Mediterranean climate in the the 21st century. *Scientific Reports*, 4, 7211. Available from: https://doi.org/10.1038/srep/07211

Allen, R.J. & Luptowitz, R. (2017) El Niño-like teleconnection increases California precipitation in response to warming. *Nature communications*, 8, 16055. Available from: https://doi.org/10.1038/ncomms16055

Banerjee, A., Fyfe, J.C., Polvani, L.M., Waugh, D. & Chang, K.-L. (2020) A pause in Southern Hemisphere circulation trends due to the Montreal protocol. *Nature*, 579, 544–548.

Betts, A.K. & Ridgway, W. (1989) Climatic equilibrium of the atmospheric convective boundary layer over a tropical ocean. *Journal of the Atmospheric Sciences*, 46, 2621–2641.

Blackport, R. & Fyfe, J.C. (2022) Climate models fail to capture strengthening wintertime North Atlantic jet and impacts on Europe. *Science Advances*, 8, eabn3112.

Burls, N.J., Blamey, R.C., Cash, B.A., Swenson, E.T., Fahad, A.A., Bopape, M.-J.M. et al. (2019) The cape town "day zero" drought and hadley cell expansion. *npj Climate and Atmospheric Science*, 2, 27.

Byrne, M.P. & O'Gorman, P.A. (2016) Understanding decreases in land relative humidity with global warming: conceptual model and GCM simulations. *Journal of Climate*, 29, 9045–9061.

Chen, G., Zhang, P. & Lu, J. (2020) Sensitivity of the latitude of the westerly jet stream to climate forcing. *Geophysical Research Letters*, 47, e2019GL086563.

Chen, P., Hoerling, M.P. & Dole, R.M. (2001) The origin of the subtropical anticyclones. *Journal of the Atmospheric Sciences*, 58, 1827–1835.

Cherchi, A., Ambrizzi, T., Behera, S., Freitas, A., Morioka, Y. & Zhou, T. (2018) The response of subtropical highs to climate change. *Current Climate Change Reports*, 4, 371–382.

Daly, C., Halbleib, M., Smith, J.I., Gibson, W.P., Doggett, M.K., Taylor, G.H. et al. (2008) Physiographically sensitive mapping of climatological temperature and precipitation across the conterminous United States. *International Journal of Climatology*, 28, 2031–2064.

Deitch, M.J., Sapundjieff, M. & Feirer, S. (2017) Characterizing precipitation variability and trends in the world's Mediterranean-climate areas. *Water*, 9, 259. Available from: https://doi.org/10.3390/w9040259

Delworth, T., Cooke, W., Naik, V., Psayter, D. & Zhang, L. (2022) A weakened AMOC may prolong greenhouse gas-induced Mediterranean drying even with significant and rapid climate change mitigation. *Proceedings of the National Academy of Sciences of the United States of America*, 119, e2116655119. Available from: https://doi.org/10.1073/pnas.2116655119

Dong, L. & Leung, L.R. (2021) Winter precipitation changes in California under global warming: contributions of CO_2, uniform SST warming, and SST change patterns. *Geophysical Research Letters*, 48, e2020GL091736.

Dong, L., Leung, L.R., Lu, J. & Song, F. (2019) Mechanisms for an amplified precipitation seasonal cycle in the US West Coast under global warming. *Journal of Climate*, 32, 4681–4698.

Eyring, V., Bony, S., Meehl, G., Senior, C., Stevens, B., Stouffer, R. et al. (2016) Overview of the Coupled Model Intercomparison Project Phase 6 (CMIP6) experimental design and organization. *Geoscientific Model Development*, 9, 1937–1958.

Fogt, R.L. & Marshall, G.J. (2020) The southern annular mode: variability, trends, and climate impacts across the Southern Hemisphere. *Wiley Interdisciplinary Reviews: Climate Change*, 11, e652.

Frierson, D.M.W., Lu, J. & Chen, G. (2007) Width of the Hadley Cell in simple and comprehensive general circulation models. *Geophysical Research Letters*, 34, L18804. Available from: https://doi.org/10.1029/2007GL031115

Garfinkel, C.I., Adam, O., Morin, E., Enzel, Y., Elbaum, E., Bartov, M. et al. (2020) The role of zonally averaged climate change in contributing to intermodel spread in CMIP5

predicted local precipitation changes. *Journal of Climate*, 33, 1141–1154.

Garreaud, R.D., Alvarez-Garreton, C., Barichivich, J., Boisier, J.P., Christie, D., Galleguillos, M. et al. (2018) The 2010–2015 megadrought in central Chile: impacts on regional hydroclimate and vegetation. *Hydrology and Earth System Sciences*, 21, 6307–6327.

Goss, M., Swain, D.L., Abatzoglou, J.T., Sarhadi, A., Kolden, C.A., Williams, A.P. et al. (2020) Climate change is increasing the likelihood of extreme autumn wildfire conditions across California. *Environmental Research Letters*, 15, 094016.

Grise, K.M., Davis, S., Simpson, I., Waugh, D., Fu, Q., Allan, R. et al. (2019) Recent tropical expansion: natural variability or forced response? *Journal of Climate*, 32, 1551–1571. Available from: https://doi.org/10.1175/JCLI–D–18–0444.1

Grise, K.M. & Polvani, L.M. (2011) The response of mid-latitude jets to increased CO_2: distinguishing the roles of sea surface temperature and direct radiative forcing. *Geophysical Research Letters*, 41, 6863–6871. Available from: https://doi.org/10.1002/2014GL061638

Harris, I., Osborn, T.J., Jones, P. & Lister, D.H. (2020) Version 4 of the CRU TS monthly high-resolution gridded multivariate climate dataset. *Scientific Data*, 7, 109. Available from: https://doi.org/10.1038/s41597-020-0453-3

Hawkins, E. & Sutton, R. (2009) The potential to narrow uncertainty in regional climate predictions. *Bulletin of the American Meteorological Society*, 90, 1095–1108.

Hawkins, E. & Sutton, R. (2011) The potential to narrow uncertainty in projections of regional precipitation change. *Climate Dynamics*, 37, 407–418.

He, C., Wu, B., Zou, L. & Zhou, T. (2017) Responses of the summertime subtropical anticyclones to global warming. *Journal of Climate*, 30, 6465–6479. Available from: https://doi.org/10.1175/JCLI-D-16-0529.1

Heede, U.K. & Federov, A. (2023) Colder eastern equatorial Pacific and stronger Walker circulation in the early 21st century: separating the forced response to global warming from natural variability. *Geophysical Research Letters*, 50, e2022GL101020. Available from: https://doi.org/10.1029/2022GL101020

Hersbach, H., Bell, B., Berrisford, P., Hirahara, S., Horanyi, A., Munoz-Sabatez, J. et al. (2020) The ERA5 global reanalysis. *Quarterly Journal of the Royal Meteorological Society*, 146, 1999–2049.

Hoerling, M.P., Eischeid, J., Kumar, A., Leung, R., Mariotti, A., Mo, K. et al. (2014) Causes and predictability of the 2012 Great Plains drought. *Bulletin of the American Meteorological Society*, 95, 269–282.

Hoskins, B. & Valdes, P.J. (1990) On the existence of storm tracks. *Journal of the Atmospheric Sciences*, 47, 1854–1864.

Jacobson, T.W., Seager, R., Williams, A. & Henderson, N. (2022) Climate dynamics preceding summer forest fires in California and the extreme case of 2018. *Journal of Applied Meteorology and Climatology*, 61, 989–1002.

Jacobson, T.W., Seager, R., Williams, A., Simpson, I., MacKinnon, K. & Liu, H. (2023) An unexpected decline in spring atmospheric humidity in the interior southwestern United States and implications for forest fires. *Journal of Hydrometeorology*, 25, 373–390.

Jones, M.W., Abatzoglou, J.T., Veraverbeke, S., Andela, N., Lasslop, G., Forkel, M. et al. (2022) Global and regional trends and drivers of fire under climate change. *Reviews of Geophysics*, 60, e2020RG000726.

Kelley, C., Ting, M., Seager, R. & Kushnir, Y. (2012) Mediterranean precipitation climatology, seasonal cycle, and trend as simulated by CMIP5. *Geophysical Research Letters*, 39, L21703. Available from: https://doi.org/10.1029/2012GL053416

Kelley, C., Ting, M., Seager, R. & Kushnir, Y. (2011) The relative contributions of radiative forcing and internal climate variability to the late 20th century winter drying of the Mediterranean region. *Climate Dynamics*, 38, 2001–2015. Available from: https://doi.org/10.1007/s00382-011-1221-z

Lee, S., L'Heureux, M., Wittenberg, A., Seager, R., O'Gorman, A. & Johnson, N. (2022) On the future zonal contrasts of equatorial Pacific climate: perspectives from observations, simulation and theories. *npj Climate and Atmospheric Science*, 5, 82. Available from: https://doi.org/10.1038/s41612-022-00301-2

Leemans, R. & Cramer, W.P. (1991) *The IIASA database for mean monthly values of temperature, precipitation, and cloudiness on a global terrestrial grid*. Laxenburg: IIASA. Technical report RR-91-018.

Lehner, F., Deser, C., Maher, N., Marotzke, J., Fischer, E.M., Brunner, L. et al. (2020) Partitioning climate projection uncertainty with multiple large ensembles and CMIP5/6. *Earth System Dynamics*, 11, 491–508.

Lionello, P., Bhend, J., Buzzi, A., Della-Marta, P., Krichak, S.O., Jansa, A. et al. (2006) Cyclones in the Mediterranean region: climatology and effects on the environment. In: Lionello, P., Malanotte-Rizzoli, P. & Boscolo, R. (Eds.) *Mediterranean climate variability*. Amsterdam: Elsevier, pp. 325–372.

Lu, J., Chen, G. & Frierson, D.M.W. (2008) Response of the zonal mean atmospheric circulation to El Niño versus global warming. *Journal of Climate*, 21, 5835–5851.

Lukovic, J., Chiang, J., Blagojevic, D. & Sekulic, A. (2021) A later onset of the rainy season in California. *Geophysical Research Letters*, 48, e2020GL090350. Available from: https://doi.org/10.1029/2020GL090350

Maher, N., Kay, J.E. & Capotondi, A. (2022) Modulation of ENSO teleconnections over North America by the Pacific decadal oscillation. *Environmental Research Letters*, 17, 114005.

McLandress, C., Shepherd, T., Scinocca, J., Plummer, D., Sigmond, M., Jonsson, A. et al. (2011) Separating the dynamical effects of climate change and ozone depletion. Part II: Southern Hemisphere troposphere. *Journal of Climate*, 24, 1850–1868.

Olonscheck, D., Rugenstein, M. & Marotzke, J. (2020) Broad consistency between observed and simulated trends on sea surface temperature patterns. *Geophysical Research Letters*, 47, e2019GL086773. Available from: https://doi.org/10.1029/2019/GL086773

Pascale, S., Kapnick, S.B., Delworth, T.L. & Cooke, W.F. (2020) Increasing risk of another cape town "day zero" drought in the 21st century. *Proceedings of the National Academy of Sciences of the United States of America*, 117, 29495–29503.

Polade, S.D., Gershunov, A., Cayan, D.R., Dettinger, M.D. & Pierce, D.W. (2017) Precipitation in a warming world: assessing projected hydro-climate changes in California and other Mediterranean climate regions. *Scientific Reports*, 7, 10783. Available from: https://doi.org/10.1038/s41598-017-11285-y

Polvani, L.M., Waugh, D.W., Correa, G.J.P. & Son, S. (2011) Stratospheric ozone depletion: the main driver of 20th century

atmospheric circulation changes in the Southern Hemisphere. *Journal of Climate*, 24, 795–812. Available from: https://doi.org/10.1175/2010JCLI3772.1

Rodwell, M.J. & Hoskins, B.J. (2001) Subtropical anticyclones and summer monsoons. *Journal of Climate*, 14, 3192–3211.

Schneider, U., Becker, A., Finger, P., Meyer-Christoffer, A., Ziese, M. & Rudolf, B. (2014) GPCC's new land surface precipitation climatology based on quality-controlled in situ data and its role in quantifying the global water cycle. *Theoretical and Applied Climatology*, 115, 15–40.

Seager, R., Cane, M.A., Henderson, N., Lee, D., Abernathey, R. & Zhang, H. (2019a) Strengthening tropical Pacific zonal sea surface temperature gradient consistent with rising greenhouse gases. *Nature Climate Change*, 9, 517–522.

Seager, R., Harnik, N., Robinson, W.A., Kushnir, Y., Ting, M., Huang, H.P. et al. (2005) Mechanisms of ENSO-forcing of hemispherically symmetric precipitation variability. *Quarterly Journal of the Royal Meteorological Society*, 131, 1501–1527.

Seager, R., Henderson, N. & Cane, M.A. (2022a) Persistent discrepancies between observed and modeled trends in the tropical Pacific Ocean. *Journal of Climate*, 35, 4571–4584.

Seager, R., Hoerling, M., Schubert, S., Wang, H., Lyon, B., Kumar, A. et al. (2015) Causes of the 2011–14 California drought. *Journal of Climate*, 28, 6997–7024.

Seager, R., Liu, H., Henderson, N., Simpson, I., Kelley, C., Shaw, T. et al. (2014) Causes of increasing aridification of the Mediterranean region in response to rising greenhouse gases. *Journal of Climate*, 27, 4655–4676.

Seager, R., Murtugudde, R., Naik, N., Clement, A., Gordon, N. & Miller, J. (2003) Air–sea interaction and the seasonal cycle of the subtropical anticyclones. *Journal of Climate*, 16, 1948–1966.

Seager, R., Osborn, T.J., Kushnir, Y., Simpson, I.R., Nakamura, J. & Liu, H. (2019b) Climate variability and change of Mediterranean-type climates. *Journal of Climate*, 32, 2887–2915.

Seager, R., Ting, M., Alexander, P., Nakamura, J., Liu, H., Li, C. et al. (2023) Ocean-forcing of cool season precipitation drives ongoing and future decadal drought in southwestern North America. *npj Climate and Atmospheric Science*, 6, 141.

Seager, R., Ting, M., Alexander, P., Nakamura, J., Liu, H., Li, C. et al. (2022b) Mechanisms of a meteorological drought onset: summer 2020 to spring 2021 in southwestern North America. *Journal of Climate*, 35, 3767–3785.

Shaw, T.A. (2019) Mechanisms of future predicted changes in the zonal mean mid-latitude circulation. *Current Climate Change Reports*, 5, 345–357.

Shepherd, T.G. (2014) Atmospheric circulation as a source of uncertainty in climate change projections. *Nature Geoscience*, 7, 703–708.

Shiogama, H., Fujimori, S., Hasegawa, T., Hayashi, M., Hirabayashi, Y., Ogura, T. et al. (2023) Important distinctiveness of SSP3-7.0 for use in impact assessments. *Nature Climate Change*, 13, 1276–1278.

Simpson, I., McKinnon, K., Kennedy, D., Lawrence, D., Lehner, F. & Seager, R. (2023) Observed humidity trends in dry regions are inconsistent with climate models. *Proceedings of the National Academy of Sciences of the United States of America*, 121(1), e2302480120.

Simpson, I., Seager, R., Shaw, T. & Ting, M. (2015) Mediterranean summer climate and the importance of Middle East topography. *Journal of Climate*, 28, 1977–1996.

Simpson, I., Seager, R., Ting, M. & Shaw, T.A. (2016) Causes of change in Northern Hemisphere winter meridional wind and regional hydroclimate. *Nature Climate Change*, 6, 65–70. Available from: https://doi.org/10.1038/NCLIMATE2783

Simpson, I., Shaw, T. & Seager, R. (2014) A diagnosis of the seasonally and longitudinally varying mid-latitude circulation response to global warming. *Journal of the Atmospheric Sciences*, 71, 2489–2515.

Solomon, S., Ivy, D.J., Kinnison, D., Mills, M.J., Neely, R.R., III & Schmidt, A. (2016) Emergence of healing in the Antarctic ozone layer. *Science*, 353, 269–274.

Sousa, P.M., Blamey, R.C., Reason, C.J., Ramos, A.M. & Trigo, R.M. (2018) The day zero cape town drought and the poleward migration of moisture corridors. *Environmental Research Letters*, 13, 124025.

Swain, D., Tsiang, M., Haughen, M., Singh, D., Charland, A., Rajarthan, B. et al. (2014) The extraordinary California drought of 2013/14: character, context and the role of climate change. *Bulletin of the American Meteorological Society*, 95, S3–S6.

Swain, D.L. (2021) A shorter, sharper rainy season amplifies California wildfire risk. *Geophysical Research Letters*, 48, e2021GL092843.

Thompson, D.W.J., Solomon, S., Kushner, P.J., England, M.H., Grise, K.M. & Karoly, D.J. (2011) Signatures of the Antarctic ozone hole in Southern Hemisphere surface climate change. *National Geographic*, 4, 741–749.

Ting, M., Seager, R., Li, C., Liu, H. & Henderson, N. (2018) Mechanisms of future spring drying in the southwestern United States in CMIP5 models. *Journal of Climate*, 31, 4265–4279.

Trigo, I.F., Pozo-Vazquez, D., Osborn, T.J., Castro-Diez, Y., Gamiz-Fortis, S. & Esteban-Parra, M.J. (2004) North Atlantic oscillation influence on precipitation, river flow and water resources in the Iberian peninsula. *International Journal of Climatology*, 24, 925–944.

Tuel, A. & Eltahir, E.A. (2020) Why is the Mediterranean a climate change hot spot? *Journal of Climate*, 33, 5829–5843.

Tuel, A. & Eltahir, E.A. (2021) Mechanisms of European summer drying under climate change. *Journal of Climate*, 34, 8913–8931.

Tuel, A., O'Gorman, P.A. & Eltahir, E.A. (2021) Elements of the dynamical response to climate change over the Mediterranean. *Journal of Climate*, 34, 1135–1146.

Watanabe, M., Dufresne, J., Kosaka, Y., Mauritsen, T. & Tatebe, H. (2020) Enhanced warming constrained by past trends in equatorial Pacific sea surface temperature gradient. *Nature Climate Change*, 11, 33–37. Available from: https://doi.org/10.1038/s41558-020-00933-3

Watt-Meyer, O., Frierson, D.M. & Fu, Q. (2019) Hemispheric asymmetry of tropical expansion under CO_2 forcing. *Geophysical Research Letters*, 46, 9231–9240.

Williams, A.P., Abatzoglu, J., Gershunov, A., Guzman-Morales, J., Bishop, D.A., Balch, J. et al. (2019) Observed impacts of anthropogenic climate change on wildfire in California. *Earth's Future*, 7, 892–910. Available from: https://doi.org/10.1029/2019EF001210

Williams, A.P., Seager, R., Macalady, A.K., Berkelhammer, M., Crimmins, M.A., Swetnam, T.W. et al. (2015) Correlations between components of the water balance and burned area reveal new insights for predicting forest-fire area in the southwest United States. *International Journal of Wildland Fire*, 24, 14–26.

Wills, R., Dong, Y., Proistosecu, C., Armour, K. & Battisti, D. (2022) Systematic climate model biases in the large-scale patterns of recent sea-surface temperature and sea-level pressure change. *Geophysical Research Letters*, 49, e2022GL100011. Available from: https://doi.org/10.1029/2022GL100011

Wu, Y., Polvani, L. & Seager, R. (2013a) The importance of the Montreal protocol for protecting the Earth's hydroclimate. *Journal of Climate*, 26, 4049–4068.

Wu, Y., Seager, R., Ting, M., Naik, N. & Shaw, T. (2012) Atmospheric circulation response to an instantaneous doubling of carbon dioxide. Part I: model experiments and transient thermal response in the troposphere. *Journal of Climate*, 25, 2862–2879.

Wu, Y., Seager, R., Ting, M., Naik, N. & Shaw, T. (2013b) Atmospheric circulation response to an instantaneous doubling of carbon dioxide. Part II: atmospheric transient adjustment and its dynamics. *Journal of Climate*, 26, 918–935.

Xoplaki, E., Gonzalez-Rouco, J.F. & Luterbacher, J. (2004) Wet season Mediterranean precipitation variability: influence of large-scale dynamics and trends. *Climate Dynamics*, 23, 63–78.

Zappa, G., Hawcroft, M.K., Shaffrey, L.C., Black, E. & Brayshaw, D.J. (2015a) Extratropical cyclones and the projected decline of winter Mediterranean precipitation in the CMIP5 models. *Climate Dynamics*, 45, 1727–1738. Available from: https://doi.org/10.1007/s00382-014-2426-8

Zappa, G., Hoskins, B.J. & Shepherd, T.G. (2015b) The dependence of wintertime Mediterranean precipitation on the atmospheric circulation response to climate change. *Environmental Research Letters*, 10, 104012. Available from: https://doi.org/10.1088/1748-9326/10/12/129501

How to cite this article: Seager, R., Wu, Y., Cherchi, A., Simpson, I. R., Osborn, T. J., Kushnir, Y., Lukovic, J., Liu, H., & Nakamura, J. (2024). Recent and near-term future changes in impacts-relevant seasonal hydroclimate in the world's Mediterranean climate regions. *International Journal of Climatology*, *44*(11), 3792–3820. https://doi.org/10.1002/joc.8551